

How Much Progress Has There Been in NVIDIA Datacenter GPUs?

Emanuele Del Sozzo, Martin Fleming, Kenneth Flamm, and Neil Thompson

Abstract—Graphics Processing Units (GPUs) are the state-of-the-art architecture for essential tasks, ranging from rendering 2D/3D graphics to accelerating workloads in supercomputing centers and, of course, Artificial Intelligence (AI). As GPUs continue improving to satisfy ever-increasing performance demands, analyzing past and current progress becomes paramount in determining future constraints on scientific research. This is particularly compelling in the AI domain, where rapid technological advancements and fierce global competition have led the United States to recently implement export control regulations limiting international access to advanced AI chips. For this reason, this paper studies technical progress in NVIDIA datacenter GPUs released from the mid-2000s until today. Specifically, we compile a comprehensive dataset of datacenter NVIDIA GPUs comprising several features, ranging from computational performance to release price. Then, we examine trends in main GPU features and estimate progress indicators for per-memory bandwidth, per-dollar, and per-watt increase rates. Our main results identify doubling times of 1.44 and 1.69 years for FP16 and FP32 operations (without accounting for sparsity benefits), while FP64 doubling times range from 2.06 to 3.79 years. Off-chip memory size and bandwidth grew at slower rates than computing performance, doubling every 3.32 to 3.53 years. The release prices of datacenter GPUs have roughly doubled every 5.1 years, while their power consumption has approximately doubled every 16 years. Finally, we quantify the potential implications of current U.S. export control regulations in terms of the potential performance gaps that would result if implementation were assumed to be complete and successful. We find that recently proposed changes to export controls would shrink the potential performance gap from 23.6× to 3.54×.

Index Terms—NVIDIA Graphics Processing Units (GPUs), progress trends, growth rates, doubling times, export control.

I. INTRODUCTION

THE growing need for computational power dedicated to graphics rendering motivated the the creation of the specialized hardware we commonly call Graphics Processing Units (GPUs). Initially designed for to 2D/3D graphics and gaming, GPUs became a performant architecture to accelerate highly parallel workloads. According to the June 2025 TOP500 list [1], all five of the world’s top supercomputers employ GPUs. Moreover, GPUs have also become the *de facto* standard for the training and inference of Artificial Intelligence (AI) models, transforming the computer science field and downstream industrial markets [2], [3]. Indeed, as the central core of AI operations can be reduced to matrix/vector multiplications, the massively parallel architecture of GPUs makes them more suitable and efficient for such computations than Central Processing Units (CPUs). The role of GPUs

Emanuele Del Sozzo, Martin Fleming, Kenneth Flamm, and Neil Thompson are with MIT FutureTech, Computer Science and Artificial Intelligence Laboratory (CSAIL), Massachusetts Institute of Technology, 02139, Cambridge, MA, USA. E-mail: {delsozzo, marti264, kflamm, neil_t}@mit.edu

(and AI chips in general) has become so critical in the current intense global competition over AI development that U.S. national security policy has introduced export control regulations, intended to restrict access to advanced AI chips by certain countries [4]–[8].

GPU hardware improvements have been a key factor in the current AI revolution, alongside improved algorithms and larger datasets [9]. As the characteristics and requirements of large-scale AI models increase at impressive rates (e.g., computing demand doubles every 6 to 10 months [10], [11] and the longest context windows grow by 30× per year [12]), the GPU landscape has changed substantially at both the software and hardware levels to keep sustaining AI progress. Over the years, GPU vendor NVIDIA released highly optimized AI software libraries (e.g., CuDNN and Transformer Engine) within its Compute Unified Device Architecture (CUDA) framework. NVIDIA also integrated AI-oriented hardware functionality inside its GPUs, such as 16-bit Floating Point (FP16) units and Tensor Cores, alongside standard compute units for 32-bit Floating Point (FP32) and 64-bit Floating Point (FP64). The improved performance is now measured in Tera Floating Point Operations per Second (TFLOPS) [13]. These innovations demonstrate how domain specialization became a viable pathway, at least temporarily, to continued performance improvement [14]–[17] and performance “scaling laws” (e.g., Huang’s law for AI [18]). In contrast to the empirical record for CPU performance during the heyday of Moore’s Law and Dennard scaling in the late twentieth century [19], performance improvements and new computing features for GPUs have generally come at the cost of greater energy use and higher prices for modern GPUs. For instance, if we compare top server-/datacenter-class CPUs and GPUs from 2025 (e.g., Intel Xeon 6978P [20], AMD Ryzen Threadripper PRO 9995WX [21], and Blackwell Ultra B300 [22]), the NVIDIA device is 2.2× to 3.1× more power hungry and almost 5× more expensive than Intel and AMD devices.¹ These continuous innovations at the software and hardware levels, along with the exploding need for more (and more powerful) GPUs, made NVIDIA the *de facto* leader in this market, with a market capitalization of \$4.5 trillion in early 2026 [23]. In general, GPU users want fast turnaround times for AI training but also high precision (for instance, for scientific computing); at the same time, cutting-edge AI models are typically growing larger with billions of parameters. Consequently, analyzing the evolution of GPU generations is fundamental to finding the right balance among these conflicting demands and identifying the trade-offs NVIDIA chose to address customers’ needs.

¹This comparison uses Thermal Design Power (TDP) as a power-consumption metric. We respectively extrapolate and approximate the TDP and release price of a single B300 GPU from the available information for its HGX version.

Given the importance of GPU technical trends in current scientific fields and policy debates, this paper analyzes the pace of technical progress in NVIDIA datacenter GPUs released from the mid-2000s through 2025 and measures key trends across relevant metrics, including computing performance, size and bandwidth, power consumption, and release price. Figure 1 shows a summary of our results in terms of Compound Annual Growth Rates (CAGRs) and Doubling Times (DTs) for both a subset of the top-performing NVIDIA GPUs per year and all NVIDIA datacenter GPUs. Previous literature has examined the progress and trends of GPUs and AI hardware from various perspectives; however, these studies have important limitations. For instance, Huang’s law [18], [24] focuses on the peak computing performance across a narrow and recent set of NVIDIA GPU microarchitectures and mixes the level of precision (FP16 down to FP4), despite the reduced functionality of the smaller bitwidth systems. Not only is it implausible that such bitwidth improvements could continue, but it also leads to an inflated GPU progress estimate (nearly double what we find). Conversely, other studies [25], [26] focus on the Machine Learning (ML) and AI domains and explore a broad range of devices across vendors (e.g., NVIDIA and AMD), types (e.g., GPUs and specialized hardware), and classes (e.g., desktop, workstation, and datacenter devices). These studies also have important drawbacks. First, their analysis gives a great deal of weight to seldom-used systems, rather than the dominant platforms. They also fail to group AI-oriented (tensor) operations with others, which we argue is not the correct way to characterize performance improvements. As a consequence of these choices, they find FP16 progress rates that are 26 to 36 percentage points (ppts) lower than ours. By focusing on NVIDIA datacenter GPUs, by far the most widely used chips for AI workloads, we can simultaneously measure technical trends in an apples-to-apples comparison and provide a practical view of the rates of progress faced by most firms using AI.

Our analysis identifies the following key insights:

- Insight 1 - GPU progress surpassed Moore’s Law to keep pace with AI growth;
- Insight 2 - chip-level enhancements boosted GPU performance;
- Insight 3 - the computing power of FP16 and FP32 doubles in less than 2 years;
- Insight 4 - FP64 compute units are becoming a lower-priority resource;
- Insight 5 - HBM boosted off-chip memory size and bandwidth;
- Insight 6 - the growth in release price and TDP for best-in-class GPUs is almost 2 \times that of the datacenter lineup;
- Insight 7 - computing power grows faster than off-chip memory bandwidth;
- Insight 8 - the technical improvement per watt grows faster than the per-dollar one;
- Insight 9 - the recent update to export control regulations reduced the performance gap from 23.6 \times to 3.54 \times .

In the remainder of this paper, we first provide a simplified

architectural review of modern NVIDIA GPUs (§ II). We then report our data collection, selection, and analysis methodology (§ III). Next, we present our analysis of rates of improvement for NVIDIA GPUs, focusing first on the top-performing GPUs per year, and then on all the datacenter GPUs in our dataset (§ IV). We then examine the United States export control regulations and estimate the potential effects of such restrictions on current affected countries (§ V). We compare our work with the current literature and discuss both the limitations of our analyses and potential future research directions (§ VI). Finally, we conclude by summarizing our results (§ VII).

II. GPU ARCHITECTURE BACKGROUND

This section provides a background overview of the main architectural characteristics of NVIDIA GPUs and is intended for readers unfamiliar with NVIDIA GPU organization to facilitate the understanding of our analysis. For this reason, we organize this section into different parts that target relevant topics in NVIDIA GPU architectures.

High-Level Organization: Modern NVIDIA GPUs are computing devices implementing a two-level compute hierarchy: a parallel collection of Streaming Multiprocessors (SMs) running in Multiple Instruction Multiple Data (MIMD) mode, and SMs consisting of several heterogeneous processing cores running in Single Instruction Multiple Thread (SIMT) mode. These SIMT compute engines may be viewed as a more flexible descendant of the historical Single Instruction Multiple Data (SIMD) engine model used in earlier parallel computers and coprocessors, as they schedule processing resources to execute an identical instruction on a set of data processing threads every clock cycle. The incorporation of multiple parallel compute cores into NVIDIA GPUs roughly coincided with the historical adoption of multi-core processors in general purpose computer processor designs. The SMs compute cores can also be partitioned into separate “virtual” MIMD engines for increased programming flexibility.

Compute Units: Each SM provides hardware support for multiple instances of an instruction being executed simultaneously, with the number of configurable simultaneous Integer (INT) or Floating Point (FP) operations dependent on the arithmetic precision, which may range from low-bit precision (e.g., 16 bits) to double precision to handle operations requiring highly accurate (64-bit) results. The math processing cores are called Streaming Processors (SPs) or CUDA Cores, and an SM contains variable amounts and types of CUDA Cores depending on the GPU microarchitecture and model. For instance, SMs initially featured separated or shared CUDA Cores permitting only 32-bit integer, FP32, and FP64 operations. Then, beginning with the microarchitecture codenamed Pascal in 2016, NVIDIA introduced hardware support for FP16 within FP32 CUDA Cores in order to support AI applications, which previously utilized lower precision only through software emulation. Generally, FP16 calculations are faster and less area-demanding than FP32 operations and also require half the memory. In addition, in SMs from the Volta microarchitecture (2017) and following microarchitectures, NVIDIA added specialized Tensor Cores alongside CUDA

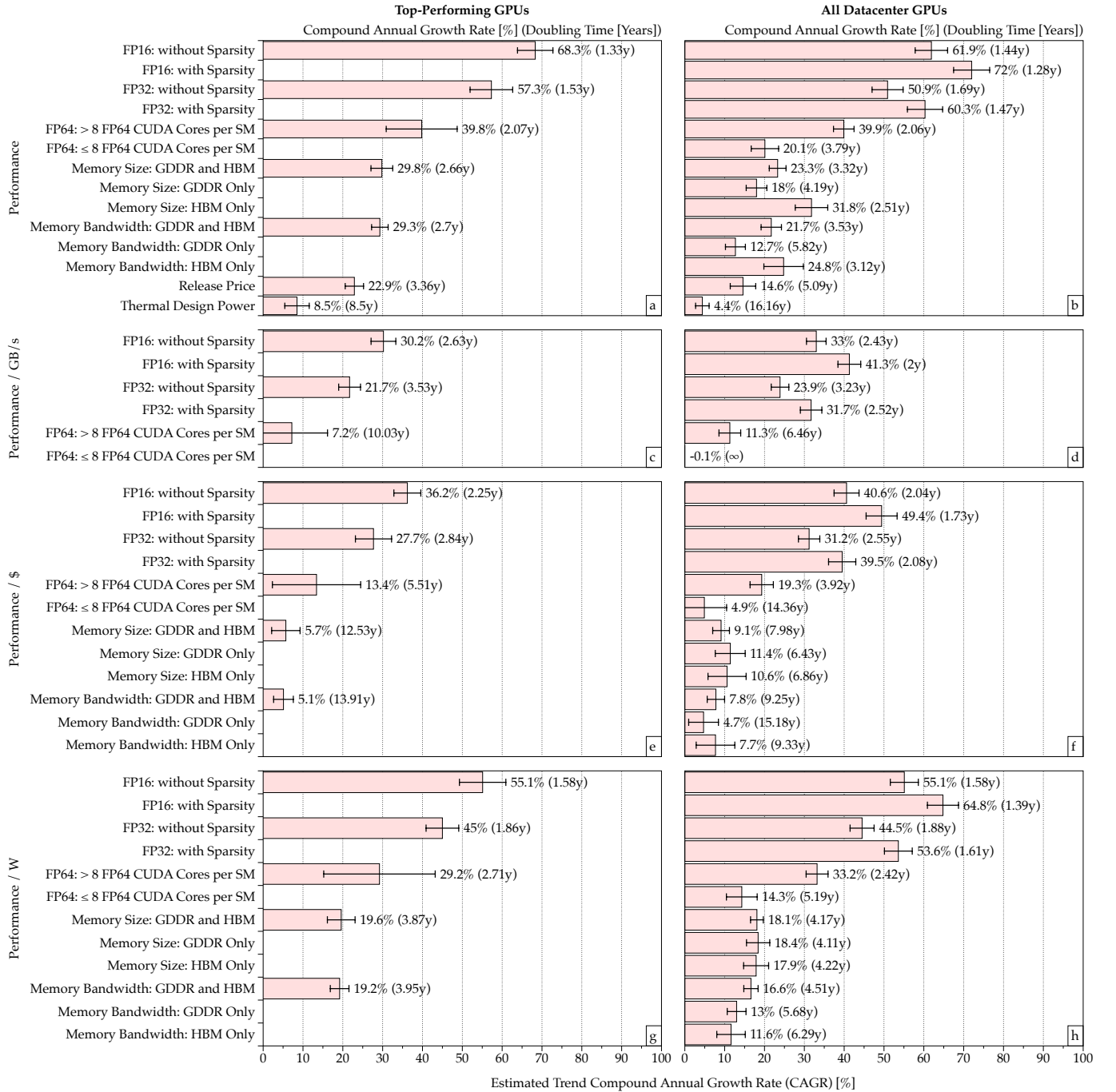


Fig. 1: Compound Annual Growth Rates (CAGRs) with 90 percent confidence intervals and Doubling Times (DTs) for computing performance, namely 16-bit Floating Point (FP16), 32-bit Floating Point (FP32), and 64-bit Floating Point (FP64), off-chip memory size and bandwidth, release price, and Thermal Design Power (TDP) deriving from technical improvements (subplots *a* and *b*) and their per-memory bandwidth (*c* and *d*), per-dollar (*e* and *f*), and per-watt (*g* and *h*) ratios for top-performing GPUs (left column) and all datacenter GPUs (right column). The Figure also accounts for the impact of sparsity (FP16 and FP32) and differentiates between GPUs with a high/low number of FP64 CUDA Cores per Streaming Multiprocessor (SM). Similarly, it shows the separate and joint contributions of GDDR and HBM technologies on memory size and bandwidth.

Cores to accelerate tensor computations, which are frequently used in the AI domain, through several Multiply–Accumulate (MAC) operations per clock cycle.² While Tensor Cores initially only supported FP16 operations, they can now execute computations at various data precisions, including 4-bit Integer (INT4), 16-bit Brain Floating Point (BF16) (also supported by recent CUDA Cores), TensorFloat-32 (TF32), and FP64. Additionally, they implement hardware support for sparse matrices at specific data precisions, which can significantly accelerate computations in certain AI applications.³ Moreover, SMs include texture units to accelerate storage and retrieval of pixel characteristics in images or simulations and Ray Tracing (RT) Cores (in some datacenter GPUs) to accelerate calculations of pixel characteristics in images or simulations. Finally, a few NVIDIA devices combine both a GPU and a Data Processing Unit (DPU) [27] on the same board, resulting in a converged acceleration card for computing and networking [28], [29].

On-Chip and Off-Chip Memory: NVIDIA GPUs feature different types of on-chip and off-chip memory. Each SM includes internal registers, with a specific number of registers assigned to each scheduled thread, a Level zero (L0) instruction cache, and a combined Level one (L1) data cache and shared memory, enabling low latency and high bandwidth data exchange between threads. Each SM can also access off-chip memory through on-chip memory controller units. Off-chip memory Dynamic Random Access Memory (DRAM) can either have a very wide interface and very low latency, provided by High Bandwidth Memory (HBMx), or less performant but less expensive solutions, such as Graphics Double Data Rate (GDDRx) memory, where the trailing “x” is the version of the industry standard. Starting with the 2016 Pascal microarchitecture, NVIDIA began to employ HBM technology for the off-chip memories of their datacenter GPUs, while desktop/workstation GPUs still rely on GDDR-based memories (e.g., the Turing and Ada microarchitectures, as well as some Ampere chips). The most current and fastest version of HBM is HBM3E, while the most advanced GDDR memory in volume production is GDDR6X, with GDDR7 coming into volume production in the near future [30]. The memory interface width and the memory interface standard used determine theoretical off-chip memory bandwidth. In general, the two primary high-level characteristics that define the off-chip memory are its size/capacity and bandwidth. The former indicates the number of bytes the off-chip memory can store; the latter indicates how quickly bytes can be transferred between the off-chip memory and the computing chip. These features are particularly relevant in applications whose performance is bounded by off-chip memory capabilities, as such applications require storing large amounts of data in off-chip memory and frequently transferring data to/from the computing chip.

²Tensor computation refers to the mathematical operations and manipulations performed on tensors, namely multidimensional arrays of data.

³Data sparsity denotes the condition in which a large proportion of data in a dataset is zero, null, or missing. The structured sparsity supported by NVIDIA GPUs requires a 2:4 sparsity pattern, where at least 2 values in each contiguous group of 4 must be zero (50% sparsity rate).

GPU Chip: As the size of GPU chips keeps growing, often approaching the limits of current chip fabrication technology, NVIDIA decided to move from a single-die (or single-chip) to a multi-die approach for its Blackwell microarchitecture (2024) and subsequent microarchitectures [31]. Similarly, NVIDIA also developed “superchips” that combine a Grace CPU with one or two GPUs [32], [33] and can potentially operate as standalone systems (with NVIDIA’s computing software stacks running on the Grace CPU) or in combination with other superchips. Actually, this is not the first time that NVIDIA has gone down this multi-die path for its GPUs, as some Kepler (2012) and Maxwell (2015) boards (i.e., K10, K80, M10, and M60) already featured multi-die GPUs. However, while dies on old GPUs, such as the K80, were connected through a relatively slow on-board Peripheral Component Interconnect Express Switch (PLX) [34], modern GPUs rely on custom, power-efficient die-to-die interfaces, namely the NVIDIA High-Bandwidth Interface (NV-HBI) [22].

Interconnect Interfaces: Each GPU (and its SMs) can communicate with other GPUs and external memory storage devices through on-board interconnect interfaces: NVLink, Peripheral Component Interconnect Express (PCIe), or Server PCI Express Module (SXM). The external interface speed affects overall computation performance in clusters of datacenter NVIDIA GPUs. Although a thorough analysis of characteristics of communication with external resources (e.g., other computing or memory devices) is beyond the scope of this paper, we will examine the critical role of the interconnection bandwidth in export control regulations (§ V).

III. DATA COLLECTION, SELECTION, AND METHODOLOGY

This section describes our data collection procedures for the class of NVIDIA GPUs we target in this work (§ III-A), explains the selection process for the metrics of interest and the top-performing GPUs per year (§ III-B), and presents the analysis methodology we employed on our curated GPU dataset to derive progress trends (§ III-C).

A. Data Collection

Our work focuses on NVIDIA, dominant in both desktop and datacenter GPU sales, with over 80% and 90% market shares, respectively [35], [36]. NVIDIA offers a broad range of GPUs with every microarchitecture covering multiple computing domains. For instance, considering only GPUs based on the Ampere microarchitecture (released in 2020 and accounting for more than 100 varieties [37]), we find both mobile and desktop solutions (e.g., GeForce 30 series [38]) and datacenter products (e.g., NVIDIA A100 [39]). Given this variety of devices, we focus on the datacenter class for two reasons: first, this choice reduces variability within the collected metrics associated with product differentiation targeting consumer graphics and display applications (vs. parallel computation in commercial and industrial applications). Second, datacenter GPUs are a better indicator of computing innovation, since higher priced products are more likely to embody novel architectural enhancements.

TABLE I: Collected datacenter GPUs in our dataset

Microarchitecture Name	First Release	GPU Model [†]
Tesla	2006	C870*, C1060*, C1080, M1060*
Fermi	2010	C2050, C2070, C2075, C2090*, M2050, M2070, M2070Q, M2075, M2090, X2070, X2090
Kepler	2012	K8, K10*, K20c, K20m, K20s, K20X, K20Xm, K40c*, K40d, K40m, K40s, K40st, K40t, K80*
Maxwell	2014	M4, M10, M40, M60*
Pascal	2016	P4, P10, P40, P100*, P100 DGXS
Volta	2017	PG500-216, PG503-216, V100*, V100 DGXS, V100 FHHL, V100S*
Turing	2018	T10, T4, T4G, T40
Ampere	2020	A2, A10, A10G, A10M, A16, A30, A30X, A40, A100*, A100X*, A800, AX800, PG506-207, PG506-217, PG506-232, PG506-242
Ada	2022	L2, L4, L20, L40, L40G, L40S, L40 CNX
Hopper	2022	H20, H100*, H100 CNX, H100 NVL*, H200, H200 NVL, H800
Blackwell	2024	B100, B200*, RTX PRO 6000 Server
Blackwell Ultra	2025	B300*

[†]For simplicity, this list excludes GPU model variants sharing the same name but implementing different features (e.g., off-chip memory size or form factor).

*This GPU model (or its variants) is part of the top-performing GPUs per year subset.

We gathered metrics for all datacenter NVIDIA GPUs from the Tesla microarchitecture (released in 2006) to the Blackwell Ultra (released in 2025), totaling 101 GPUs.⁴ We focus on on GPU-accelerator cards that require and interact with a host CPU; we do not collect devices such as NVIDIA superchips, which can also work as standalone systems. Table I reports the model names of the GPUs in our dataset, along with the microarchitecture to which they belong and the release year of that microarchitecture. Specifically, we are interested in metrics describing the GPU chip characteristics (e.g., die size and transistor counts), microarchitecture (e.g., number of CUDA compute units and on/off-chip memory), and peak theoretical performance at different data precision (e.g., FP32). For more details about the collected metrics for each GPU, see Table II, which shows how NVIDIA introduced new features over time to address the demand for different types of data precision (e.g., FP16) and specialized compute units (e.g., Tensor Cores), mainly for AI.

We use the following data sources: online databases such as TechPowerUp [40] and VideoCardz [41] to create a list of NVIDIA datacenter GPUs; NVIDIA documentation (e.g., whitepapers and datasheets) as the primary source for technical metrics, and TechPowerUp and VideoCardz as secondary sources when the NVIDIA documentation was unavailable; and the aforementioned databases and other websites/datasets (e.g., Epoch AI [26]) to collect release prices. Unfortunately, retrieving accurate and reliable data for the target GPUs was not always possible, particularly for metrics such as initial release price. NVIDIA used to publicly release highly detailed documents describing the features of each GPU microarchitecture or specific GPU models [13], [42], [43]. However, the public documentation for the most recent microarchitec-

tures (e.g., Blackwell and Blackwell Ultra) is no longer as exhaustive as it once was, and it tends to focus on specific aspects (e.g., AI-oriented performance) rather than the full range of GPU features. Consequently, we infer some values during our data collection process to fill such gaps.⁵ Finally, we considered theoretical maximum values for computing and memory performance provided by NVIDIA. Reaching this level of performance may not always be feasible in real-world computing scenarios, but these theoretical values indicate the peak theoretical potential of the target GPUs and serve as a consistent performance indicator comparable across products and over time. Furthermore, this approach enables us to decouple and evaluate each GPU component separately, which would be unfeasible with real benchmarks.

In summary, we have built a comprehensive dataset of technical and economic metrics for datacenter GPUs. Although the analysis in this paper leverages a subset of such metrics, we believe our data collection can pave the way for further analyses in the future.

⁵For instance, if NVIDIA documentation did not report the Tensor Core MAC operations per clock cycle, we computed this value using the number of compute units and running frequency. Please note that NVIDIA documentation relies on GPU boost clock when reporting the theoretical maximum TFLOPS of CUDA/Tensor Cores at different data precisions. Moreover, Hopper GPUs also have a separate boost clock for Tensor Cores supporting all data precisions but FP64 (which relies on the GPU boost clock). The limitation of this approach will be discussed in § VI. Similarly, we extrapolated the features of B100, B200, and B300 GPUs from their respective HGX platforms (the NVIDIA HGX is a platform that integrates and interconnects multiple GPUs to accelerate different workloads [44]). Another noteworthy detail is that datacenter GPUs based on desktop/workstation-oriented microarchitectures (e.g., Turing and Ada) or boards featuring specific chips (e.g., the GA102 chip [45] inside the A40 GPU) also include additional graphics components at the cost of other computing features, as also mentioned in Section II. For example, the Ada L40 GPU features NVIDIA third-generation RT Cores and substantially fewer FP64 CUDA Cores. Consequently, we included only details relevant to general-purpose or specialized computing, not to graphics.

⁴Curiously, the term *Tesla* denoted not only the first GPU microarchitecture supporting CUDA but also the class of general-purpose GPUs until NVIDIA rebranded it into *datacenter* when releasing Ampere-based devices.

TABLE II: Collected GPU metrics/features per microarchitecture (in bold the metrics we employed in our analysis)

Metric/Feature	Tesla	Fermi	Kepler	Maxwell	Pascal	Volta	Turing	Ampere	Ada	Hopper	Blackwell	Blackwell Ultra
Chip Name	✓	✓	✓	✓	✓	✓	✓	✓	✓	✓	✓	✗
Release Year	✓	✓	✓	✓	✓	✓	✓	✓	✓	✓	✓	✓
Launch Price	✗	✗	✗	✗	✗	✗	✗	✗	✗	✗	✓	✓
Manufacturing Process	✓	✓	✓	✓	✓	✓	✓	✓	✓	✓	✓	✓
Transistor Count	✓	✓	✓	✓	✓	✓	✓	✓	✓	✓	✓	✓
Die Size	✓	✓	✓	✓	✓	✓	✓	✓	✓	✓	✗	✗
Die Density	✓	✓	✓	✓	✓	✓	✓	✓	✓	✓	✓	✗
Bus Interface	✓	✓	✓	✓	✓	✓	✓	✓	✓	✓	✓	✓
Thermal Design Power	✓	✓	✓	✓	✓	✓	✓	✓	✓	✓	✓	✓
Base Clock	✓	✓	✓	✓	✓	✓	✓	✓	✓	✗	✗	✗
Boost Clock	✓	✓	✗	✓	✓	✓	✓	✓	✗	✗	✓	✓
Streaming Multiprocessor (SM)	✓	✓	✓	✓	✓	✓	✓	✓	✓	✓	✓	✓
Processing Blocks (PBs) per SM	✓	✓	✓	✓	✓	✓	✓	✓	✓	✓	✓	✓
CUDA Cores: INT32 per PB	✓	✓	✓	✓	✓	✓	✓	✓	✓	✓	✓	✓
CUDA Cores: INT32 per SM	✓	✓	✓	✓	✓	✓	✓	✓	✓	✓	✓	✓
CUDA Cores: INT32 per GPU	✓	✓	✓	✓	✓	✓	✓	✓	✗	✗	✓	✓
CUDA Cores: FP32 per PB	✓	✓	✓	✓	✓	✓	✓	✓	✓	✓	✓	✓
CUDA Cores: FP32 per SM	✓	✓	✓	✓	✓	✓	✓	✓	✓	✓	✓	✓
CUDA Cores: FP32 per GPU	✓	✓	✓	✓	✓	✓	✓	✓	✓	✓	✓	✓
CUDA Cores: FP64 per PB	✗	✓	✓	✓	✓	✓	✓	✓	✗	✗	✗	—
CUDA Cores: FP64 per SM	✗	✓	✓	✓	✓	✓	✓	✓	✓	✓	✓	✓
CUDA Cores: FP64 per GPU	✗	✓	✓	✓	✓	✓	✓	✓	✗	✗	✓	✓
CUDA Cores: Peak FP16 Performance	—	—	—	—	✓	✓	✓	✓	✓	✓	✓	✓
CUDA Cores: Peak BF16 Performance	—	—	—	—	—	—	—	✓	✓	✓	✓	✓
CUDA Cores: Peak INT32 Performance	✓	✓	✓	✓	✓	✓	✓	✓	✓	✓	✓	✓
CUDA Cores: Peak FP32 Performance	✓	✓	✓	✓	✓	✓	✓	✓	✓	✓	✓	✓
CUDA Cores: Peak FP64 Performance	✗	✓	✓	✓	✓	✓	✓	✓	✗	✓	✓	✓
Tensor Cores: Boost Clock	—	—	—	—	—	—	—	—	—	✓	—	—
Tensor Cores: Units per PB	—	—	—	—	—	✓	✓	✓	✓	✓	✓	✓
Tensor Cores: Units per SM	—	—	—	—	—	✓	✓	✓	✓	✓	✓	✓
Tensor Cores: Units per GPU	—	—	—	—	—	✓	✓	✓	✗	✗	✓	✓
Tensor Cores: Generation	—	—	—	—	—	✓	✓	✓	✓	✓	✓	✓
Tensor Cores: FP16 MAC per Cycle	—	—	—	—	—	✓	✓	✓	✓	✓	✓	✓
Tensor Cores: Supported Data Types	—	—	—	—	—	✓	✓	✓	✓	✓	✓	✓
Tensor Cores: Sparsity Support	—	—	—	—	—	—	—	✓	✓	✓	✓	✓
Tensor Cores: Peak INT4 Performance	—	—	—	—	—	✓	✓	✓	✓	✗	✗	✗
Tensor Cores: Peak FP4 Performance	—	—	—	—	—	—	—	—	—	✓	✓	✓
Tensor Cores: Peak FP6 Performance	—	—	—	—	—	—	—	—	—	—	✓	✓
Tensor Cores: Peak INT8 Performance	—	—	—	—	—	✓	✓	✓	✓	✓	✓	✓
Tensor Cores: Peak FP8 Performance	—	—	—	—	—	—	—	—	✓	✓	✓	✓
Tensor Cores: Peak FP16 Performance	—	—	—	—	—	✓	✓	✓	✓	✓	✓	✓
Tensor Cores: Peak BF16 Performance	—	—	—	—	—	—	—	✓	✓	✓	✓	✓
Tensor Cores: Peak TF32 Performance	—	—	—	—	—	—	—	✓	✓	✓	✓	✓
Tensor Cores: Peak FP64 Performance	—	—	—	—	—	—	—	✓	—	✓	✓	✓
Register File Size per SM	✗	✓	✓	✓	✓	✓	✓	✓	✓	✓	✓	✓
Register File Size per GPU	✗	✓	✓	✓	✓	✓	✓	✓	✗	✗	✓	✓
Shared Memory Size per SM	✓	✓	✓	✓	✓	✓	✓	✓	✓	✓	✓	✓
L1 Cache Size per SM	✗	✓	✓	✓	✓	✓	✓	✓	✓	✓	✓	✓
L1 Cache Size per GPU	✓	✓	✓	✓	✓	✓	✓	✓	✓	✓	✓	✓
L2 Cache Size per GPU	✓	✓	✓	✓	✓	✓	✓	✓	✓	✓	✓	✗
Memory Type	✓	✓	✓	✓	✓	✓	✓	✓	✓	✓	✓	✓
Memory Size	✓	✓	✓	✓	✓	✓	✓	✓	✓	✓	✓	✓
Memory Bus	✓	✓	✓	✓	✓	✓	✓	✓	✓	✓	✓	✓
Memory Bandwidth	✓	✓	✓	✓	✓	✓	✓	✓	✓	✓	✓	✓
Memory Data Rate	✓	✓	✓	✓	✓	✓	✓	✓	✓	✓	✓	✓
NVLink Bandwidth	—	—	—	—	✗	✗	—	✗	—	✓	✗	✓

✓: metric/feature collected for all GPUs belonging to a given microarchitecture

✗: metric/feature collected for some GPUs belonging to a given microarchitecture (e.g., metric not available/implemented or retrievable for some GPUs)

✗: metric/feature technically available/implemented but not retrievable for any GPU belonging to a given microarchitecture

—: metric/feature not available/implemented for a given microarchitecture.

B. Data Selection

1) Metric Selection: Our analysis identifies relevant trends in GPU progress by looking at the main characteristics defining GPU performance. To this end, we focus on theoretical Floating Point (FP) computing performance, off-chip memory size and bandwidth, release price, and power consumption. We aim to analyze trends in GPU improvements from a theoretical peak perspective, without referencing specific benchmarks or AI models, which vary significantly and are unavailable for GPUs released over the entire target period (2007 to 2025). This approach allows us to consistently compare progress in

different GPU capabilities over decades. We do not distinguish between single- and multi-die GPUs in our analysis, treating the latter as a single logical GPU. We address the limitations in our analysis in § VI.

For computing performance metric, we rely on the theoretical maximum TFLOPS that GPUs can process when employing FP16, FP32, and FP64. FP16 data precision was available only through software emulation before NVIDIA introduced hardware support in the Pascal microarchitecture (2016). Hence, we approximate FP16 performance through FP32 performance for previous microarchitectures (from Tesla

to Maxwell) [9]. Hence, we use FP32 performance values to represent FP16 performance in previous microarchitectures (from Tesla to Maxwell) [9]. As described in Section II, NVIDIA introduced Tensor Cores in the Volta microarchitecture (2017) for FP16 tensor computations and later extended the support to FP32 and FP64, as well as other data precisions that we do not analyze in this study (e.g., 8-bit INT/FP precision).⁶ In addition, starting from the Ampere microarchitecture, Tensor Cores also benefit from hardware sparsity support when processing inputs featuring a 2:4 sparsity pattern (i.e., for each group of four contiguous values, at least two must be zero [46]).⁷ Conversely, since the number of FP64 CUDA Cores differs dramatically by GPU chip or microarchitecture, we sort devices into two categories based on how many FP64 processing units the model of GPU contains, and study each group's evolution separately. Specifically, we use a threshold of 8 FP64 CUDA Cores per SM to discriminate between these two categories. For instance, the GA100 [39] and GA102 [45] GPU chips contain 32 and 2 FP64 CUDA Cores per SM, respectively. Our work does not analyze lower data precisions such as FP8 and FP4. Although they are undoubtedly relevant to fields like AI [47]–[49], Tensor Cores typically execute them, meaning their performance is proportional to that of Tensor Cores for FP16. In other words, when the bitwidth halves (e.g., from 16 to 8 bits), the performance usually doubles (the opposite generally happens when the bitwidth doubles, except for FP64, whose performance decreases by roughly 16× or more because FP64 operations are not as common as lower-precision operations in the AI field).⁸ Consequently, observations for these data precisions could be extrapolated by FP16 trends.

NVIDIA GPUs mainly feature two types of off-chip memory technologies: GDDR or HBM. Older GPUs and those based on desktop/workstation-oriented microarchitectures mainly use the former technology, while pure datacenter GPUs rely on the latter. Both types of memory went through steady improvement over the years, offering increasing memory bandwidth and capacity. Our work focuses on memory size (or capacity) and theoretical maximum memory bandwidth, reporting them in Gigabytes (GB) and Gigabytes per second (GB/s), respectively, because these are the main metrics that characterize off-chip memory. To enhance comparability with published studies of computer and semiconductor price trends undertaken by government statistical agencies and academic researchers, we report original release prices in nominal (current year) US dollars in our analyses (adjustment for price inflation with the reader's price deflator of choice is easily accomplished). Finally, we employ TDP as an indicator of the GPU power consumption; TDP often equals about two-thirds of peak power draw according to one prominent computer architecture [51].

⁶Technically, Tensor Cores employ the TF32 data format for 32-bit operations. Since we are interested in the theoretical performance that both CUDA and Tensor Cores can deliver for 32-bit operations, we make no distinction between FP32 and TF32 data types and refer to both as FP32 for simplicity.

⁷Tensor Cores support sparsity up to 32-bit data precision.

⁸One exception to this pattern is the Blackwell Ultra B300, whose FP4 performance is roughly 3.1× higher than FP8 performance (14000 TFLOPS vs. 4500 TFLOPS, based on the HGX B300 specifications [50]).

2) *Top-Performing GPUs Per Year Selection*: For this subset, we pick the top-performing GPUs per year based on the average of the peak performance in FP16, FP32, and FP64, delivered using either CUDA or Tensor Cores (when available), and that include the release price.

C. Methodology

After collecting for the GPUs reported in Table I and selecting the metrics of interest (Table II), our methodology leverages a regression model to analyze the main features of datacenter GPUs. In particular, we fit the data to an exponential growth model:

$$\hat{Y} = \alpha e^{(\beta t)} \quad (1)$$

where the input variable t indicates the year, α and β are parameters in the exponential model, and the dependent variable \hat{Y} represents the estimated value of a given metrics. Taking logarithms on both sides of the equation, we have a linear model with the log of the dependent variable as a linear function of time. The estimated coefficient of time in this linear model can be transformed into point estimates of the Compound Annual Growth Rate (CAGR) — or Annual Growth Rate (AGR), since they are identical in this constant growth rate model — and Doubling Time (DT) over the entire sample data time period. Approximate robust standard errors for CAGR and DT were derived from the estimated robust standard errors of the linear model time coefficient using the delta method.⁹ We use Python, Pandas, SciPy, NumPy, and the Statsmodels [52] statistical modeling and econometrics package to compute the model coefficients and derive the estimated trend model CAGR and DT estimates through the Statsmodels' Ordinary Least Squares (OLS) regression. Moreover, we calculate the standard errors and other sample statistics (e.g., mean and standard deviation) using Scipy's Percent Point Function (PPF) and Pandas' describe function.

Given these selected metrics, we estimated log-linear exponential regression models (Equation 1) using our dataset and derived the CAGRs. Our analysis reported estimates of trend CAGRs and DTs, along with 90 percent confidence intervals, for all technical improvement metrics, and technical improvement per-memory bandwidth, per-dollar, and per-watt ratios. Non-overlapping confidence intervals are a conservative sufficient condition for rejecting the hypothesis that two parameters are actually increasing at the same rate [53]. In other words, if two statistics have non-overlapping confidence intervals, they are necessarily significantly different.

IV. GPU PROGRESS TRENDS

This section analyzes diverse GPU metrics to identify trends describing GPUs' past and current progress. We start by examining trends in a subset comprising the top-performing GPUs per year. Then, we generalize and expand our study to cover all datacenter NVIDIA GPUs released from 2007

⁹If β is the coefficient of time in this linear model, and $\hat{\sigma}_\beta$ is estimated standard error, CAGR is estimated as $e^\beta - 1$; DT is estimated as $\ln(2)/\beta$. Using the delta method, $\hat{\sigma}_\beta(CAGR) = e^\beta \hat{\sigma}_\beta$; $\hat{\sigma}(DT) = (\ln(2)/\beta^2) \hat{\sigma}_\beta$.

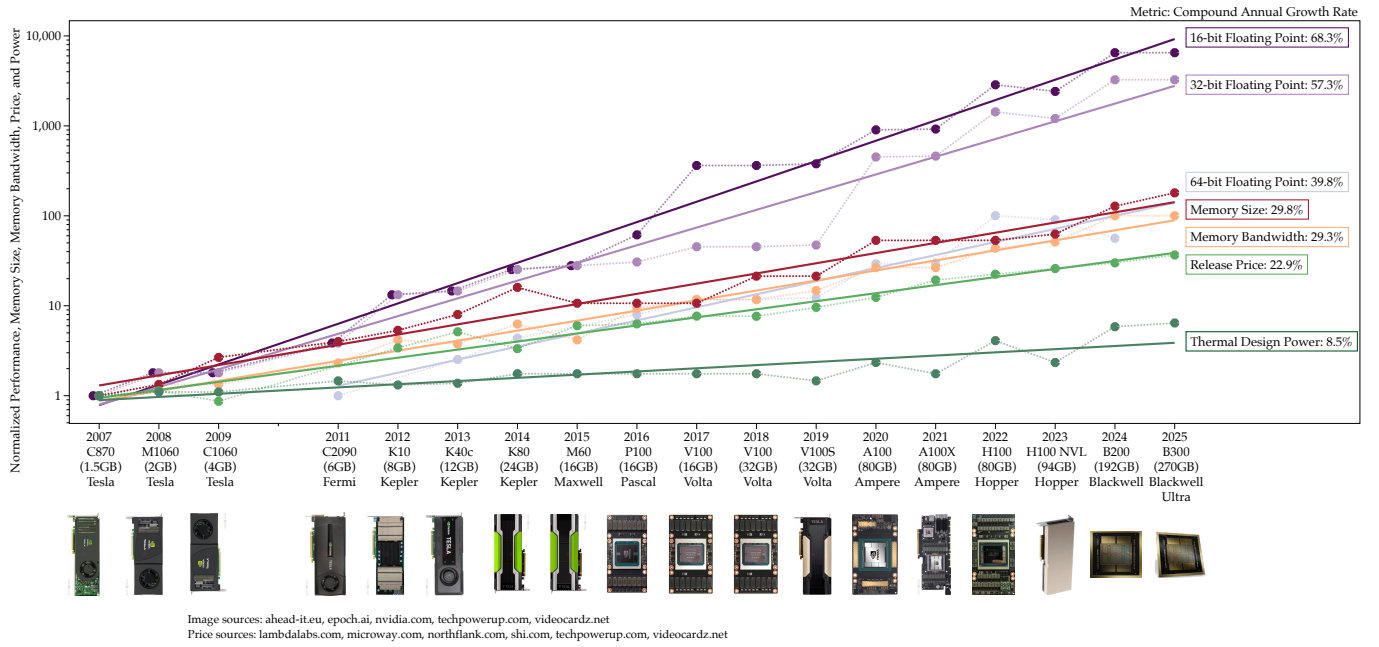


Fig. 2: **Top-performing GPUs per year:** Computing performance, off-chip memory size and bandwidth, release price, and Thermal Design Power (TDP) scaling normalized to Tesla C870. For 64-bit Floating Point (FP64), the values are normalized to Fermi C2090 (2011). The Figure also reports the estimated Compound Annual Growth Rates (CAGRs) based on exponential trends derived from the selected GPUs (solid lines) and indicates FP64 performance for GPUs with more than 8 FP64 CUDA Cores per Streaming Multiprocessor (SM). Finally, the Figure shows the GPU images and reports the off-chip memory size to help identify the specific model.

to 2025, and measure their average improvement as a group. Finally, we compare and discuss the trends across these two groups of datacenter GPUs.

A. Top-Performing GPUs Per Year

The first objective of our work is to analyze specific trends for the highest performing GPUs by year. Specifically, our analysis focuses on trends that highlight the progress of technical metrics, as well as the ratios between computational performance and memory bandwidth, release price, and power consumption. We start with this focus because we believe it is easier to identify and appreciate changes and improvements throughout the various microarchitectures of NVIDIA GPUs by concentrating on a small selection of best-in-class devices. Conceptually, these contain the maximum computing power that can be purchased in a single NVIDIA parallel computing device, at any price. For each metric, we compute both the CAGR and DT.

Given the subset of top-performing GPUs per year, we made the following assumptions and considerations to analyze major trends. Since Tensor Cores outperform CUDA Cores in tensor computations and the TFLOPS of these two processing unit types do not sum up [54], we use the former as the performance reference when available. In this way, we can observe the peak GPU performance and the transition from one type of computing resource to another. Then, to keep this analysis generalizable to a larger class of computational workloads, we do not take into account hardware sparsity support when available, and just report FP64 performance for

GPUs with numbers of FP64 CUDA Cores per SM exceeding 8.

1) *Technical Improvements:* Figure 2 shows trend lines for computational performance (FP16, FP32, and FP64), off-chip memory size and bandwidth, release price, and TDP metrics normalized to the NVIDIA Tesla C870 from 2007 (or the NVIDIA Fermi C2090 from 2011 for FP64). Introducing FP16 hardware support first (from the 2016 Pascal microarchitecture) and Tensor Cores later (from the 2017 Volta microarchitecture) boosted the performance on FP16 by roughly an order of magnitude. The 68.3% CAGR for FP16 performance, which implies a 1.33y DT, is only a little less than trend growth rates measured for Intel desktop processor performance (an average measured for all desktop CPUs, using a similar methodology) in the late 1990s, at the peak of Moore’s Law/Dennard scaling-driven performance improvement [19]. The trend for FP32 performance is similar, especially after Tensor Core support was introduced in 2020 (Ampere microarchitecture). We also observe a 39.8% CAGR for FP64, which is relatively lower than that of FP16 and FP32 and implies an estimated DT of almost 2 years. Besides, after a peak in 2022 (Hopper H100), FP64 performance has been decreasing in subsequent years, reaching a point where top-notch GPUs like the Blackwell Ultra B300 have fewer than 8 FP64 CUDA Cores per SM (which is why we do not show FP64 performance for B300 in Figure 2). Moving to other metrics, the introduction of HBM technology in GPUs (starting with the 2016 Pascal microarchitecture) significantly contributed to the growth of off-chip memory, with sharp increases in both size (29.8%

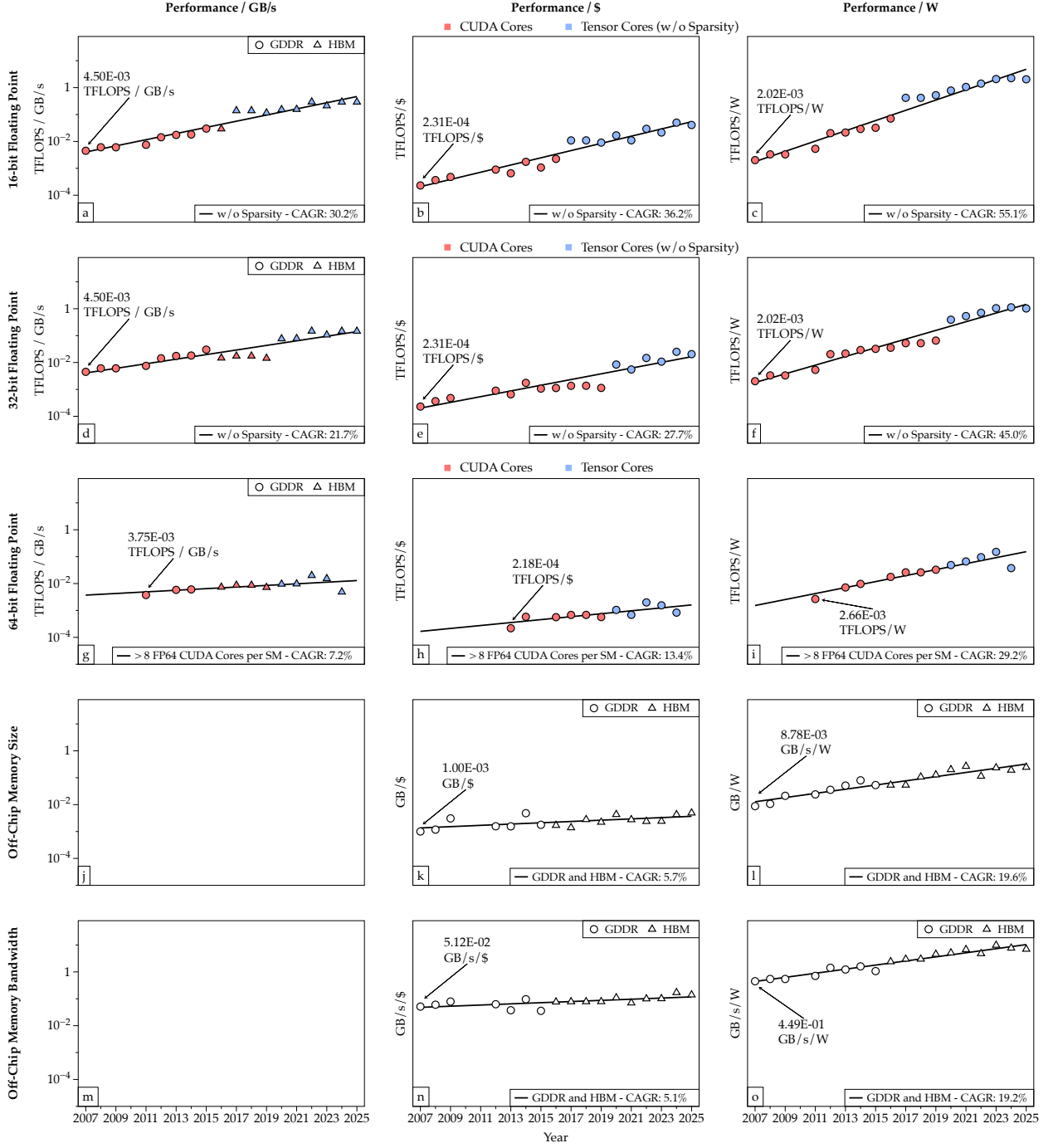


Fig. 3: **Top-performing GPUs per year:** Exponential scaling trends for the technical improvements per memory bandwidth (left column), per dollar (central column), and per watt (right column).

CAGR and 2.66y DT) and bandwidth (29.3% CAGR and 2.70y DT). Price at launch, the cost of purchasing GPUs has been consistently increasing over time, at a 22.9% CAGR from 2007 to 2025 (3.36y DT). Finally, the TDP of the selected NVIDIA GPUs grew by a much slower 8.5% every year (8.50y DT), as the 170.9W (Tesla C870) evolved into the 1100W (Blackwell Ultra B300).

2) *Technical Improvement Ratios:* After analyzing the technical improvements in the top-performing GPUs per year, we now focus on their per-memory bandwidth, per-dollar, and per-

watt ratios. Figure 3 reports the exponential scaling trends for these metrics and also indicates when the values represent CUDA/Tensor Core performance (point color in subplots *a* through *i*) or GDDR/HBM size/bandwidth (point shape in subplots *a*, *d*, *g*, *k*, *l*, *n*, and *o*).

Starting with the technical improvements per memory bandwidth (left column of plots in Figure 3), we consider only the ratio between computational performance (i.e., FP16, FP32, and FP64) and off-chip memory bandwidth, as the memory size per-bandwidth ratio essentially translates into the memory

transfer time. The FP16 per-bandwidth trend data points show the benefits Tensor Cores have provided since 2017, compensating for bandwidth improvements and resulting in a 30.2% CAGR (2.63y DT). Such a pattern is even more evident in FP32, where we can observe how HBM had been affecting trend scaling between 2016 and 2019, until the introduction of Tensor Core support for FP32 (or, rather, TF32), producing a 21.7% CAGR, which implies a 3.53y DT. Finally, the trend curve for FP64 is relatively flat (7.2% CAGR and 10.03y DT), mainly because its growth has been slower than that of FP16 and FP32. These trends generally indicate that computational performance growth tends to outpace off-chip memory bandwidth, potentially implying that the latter may become a bottleneck for computations that depend heavily on memory transfers. Consequently, this memory or bandwidth wall [55] would prevent GPUs from reaching their peak computational performance.

The central column of plots in Figure 3 illustrates the technical improvements per dollar. Starting with computational performance, we observe higher CAGRs than in the per-memory bandwidth trends. Moreover, the patterns and gaps between growth rates remain pretty similar to what we analyzed before. On the other hand, the scaling trends based on memory characteristics (i.e., size and bandwidth) per dollar are moderately flat and yield similar CAGRs (5.7% and 5.1%, respectively).

Finally, Figure 3 (right column of plots) depicts the exponential scaling trends of the technical improvements per watt. In general, we notice again patterns similar to those of the previous ratios. However, this time, the growth rates of these trends are notably higher in both computational performance and memory characteristics, due to the slower growth of TDP. Specifically, the CAGRs (DTs) range from 55.1% (1.58y) to 19.2% (3.95y) for FP16 and memory bandwidth, respectively. The gaps in growth rates across the different ratios remain roughly consistent.

B. All Datacenter GPUs

We now expand and generalize these analyses to the entire population of GPUs in our curated dataset and examine trends across all selected metrics, also considering different hardware feature configurations when available. Specifically, we focus on technical improvements for computing performance, off-chip memory size and bandwidth, release price, and TDP, as well as the per-memory bandwidth, per-dollar, and per-watt ratios. Even in this case, we estimated log-linear exponential regression models (Equation 1) and calculated CAGRs and DTs. For the performance metric, each data point represents the maximum value in terms of TFLOPS that a GPU can deliver at a given data precision. As we did in § IV-A, we replace CUDA Cores with Tensor Cores in the performance metrics as soon as the latter units become available to focus on peak theoretical performance at a given precision. On the other hand, the sparsity support within Tensor Cores (introduced in the Ampere microarchitecture) is a data-dependent feature for data precisions up to 32 bits. For this reason, we report separate exponential trend lines with and without the theoretical $2 \times$

performance improvements granted by sparsity. Instead, we fit performance for 64-bit data precision using two trend lines based on the number of FP64 CUDA Cores per SM to account for the significant performance variability across datacenter GPUs with desktop/workstation-oriented microarchitectures. Even in this analysis, we set the threshold to 8 FP64 CUDA Cores per SM. Similarly, to assess the separate contributions of GDDR and HBM to off-chip memory size and bandwidth scaling, we show decoupled trend lines for GDDR, HBM, or both. Finally, we study the exponential scaling of release prices and TDP.

1) *Technical Improvements*: Figure 4 illustrates how the technical improvements affect the estimated CAGRs of FP16, FP32, FP64, off-chip memory size and bandwidth, release price, and TDP for all NVIDIA datacenter GPUs. Figure 4 highlights the impact of sparsity (for FP16 and FP32), the amount of FP64 CUDA Cores, and different types of off-chip memory technology on the growth rates. Starting with performance metrics, FP16 and FP32 show impressive CAGRs (61.9% and 50.9% in Figure 4), which imply DTs of 1.44 years and 1.69 years, respectively. Sparsity support (dashed lines), if it can be utilized, further increases the CAGR by roughly 10 percentage points (ppts). On the other hand, FP64 performance growth varies significantly with the number of CUDA Cores per SM (from 20.1% to 39.9% in Figure 4), reflecting differences in the allocation of computing resources for this data precision across GPU microarchitectures, from pure datacenter to desktop/workstation-oriented ones. Moving to off-chip memory, we see the separate and joint contributions of GDDR and HBM technologies to the growth in memory size and bandwidth. Since its introduction in 2016 (Pascal P100), HBM (dotted lines) impacted both memory size (31.8% CAGR) and bandwidth (24.8% CAGR), outpacing GDDR (dashed lines) by roughly 14 and 12 PPTs. HBM immediately boosted memory bandwidth, as the top HBM-based bandwidth from Pascal microarchitecture (732.2GB/s in the 2016 Pascal P100 DGXS) exceeds the top GDDR-based bandwidth from the previous microarchitecture (332.8GB/s in the 2016 Maxwell M10) by more than 2X. Conversely, the initial size/capacity of HBM was smaller than that of GDDR (16GB in the 2016 Pascal P100 DGXS vs. 32GB in the 2016 Maxwell M10), so it took longer for HBM to surpass GDDR in terms of memory size. Consequently, when we analyze the joint contribution of GDDR and HBM (solid lines), we can observe that the memory size CAGR (23.3%) is closer to that of GDDR, whereas the memory bandwidth CAGR (21.7%) is closer to that of HBM.

Release prices indicate a 14.6% CAGR and a consequent 5.09y DT.¹⁰ Finally, as the maximum power that can be delivered to a PCIe-based card is \sim 300W (power demand over that requires more specialized/custom power supply, cabling, etc.), many GPUs in our dataset generally share similar TDP values ranging from 200W to 300W (60 GPUs out of 101), yielding a particularly slow growth rate for this metric (4.4%).

2) *Technical Improvement Ratios*: Figure 5 depicts the exponential scaling trends for all datacenter GPUs under

¹⁰The limitations of this analysis will be discussed in § VI.

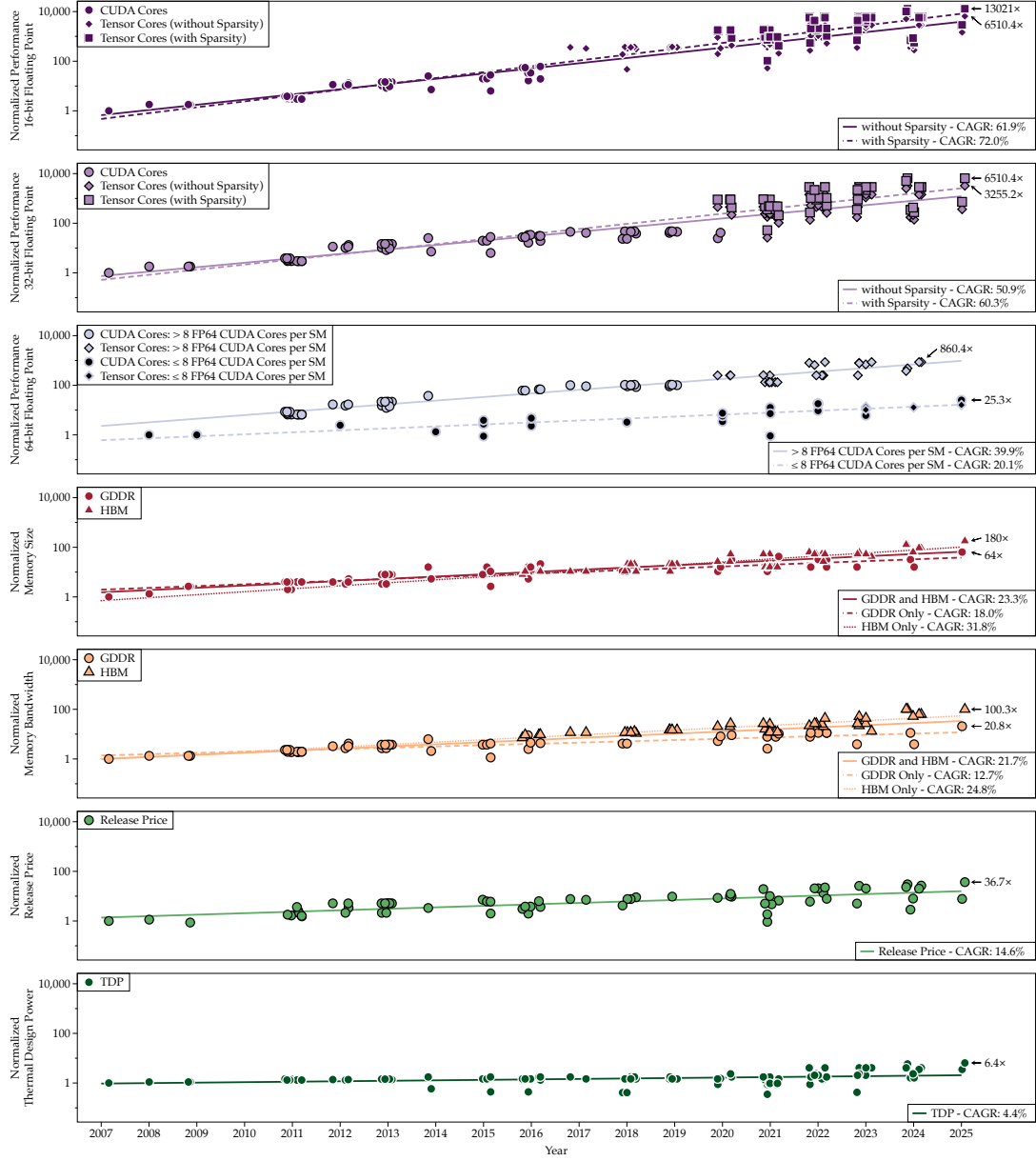


Fig. 4: **All datacenter GPUs:** Computing performance, off-chip memory size and bandwidth, release price, and Thermal Design Power (TDP) scaling normalized to Tesla C870. For 64-bit Floating Point (FP64), the values are normalized to Tesla M1060 (2008) or Fermi C2050 (2011), depending on the number of FP64 CUDA Cores per Streaming Multiprocessor (SM). The Figure also reports the estimated Compound Annual Growth Rates (CAGRs) based on exponential trends derived from the collected GPUs (solid, dashed, and dotted lines) for various configurations of computational metrics, namely 16-bit Floating Point (FP16), 32-bit Floating Point (FP32), and FP64, and memory features, namely size and bandwidth. We apply horizontal jitter to prevent overplotting.

different configurations, which include CUDA/Tensor Core performance with and without sparsity (point color in subplots from *a* through *i*), amount of FP64 CUDA Cores per SM (inner and outer point color in subplots from *g* through *i*), and GDDR/HBM size/bandwidth (point shape in subplots *a*, *d*, *g*, *l*, *n*, and *o*).

The left column of plots in Figure 5 shows the technical improvements per memory bandwidth. This specific analysis considers different configurations that affect computational performance (e.g., using CUDA Cores vs. Tensor Cores, with

or without sparsity), as these represent choices end users can make for their workloads. As HBM has been replacing GDDR as the dominant off-chip memory technology for datacenter-oriented GPU microarchitectures over the years, our analysis of technical improvements per memory bandwidth does not decouple the contributions of GDDR and HBM to highlight this transition. Nonetheless, the Figure still indicates what type of off-chip memory each point derives from. The trends for the FP16 per-memory bandwidth ratio yield CAGRs of 33.0% (without sparsity) and 41.3% (with sparsity), driven mainly by

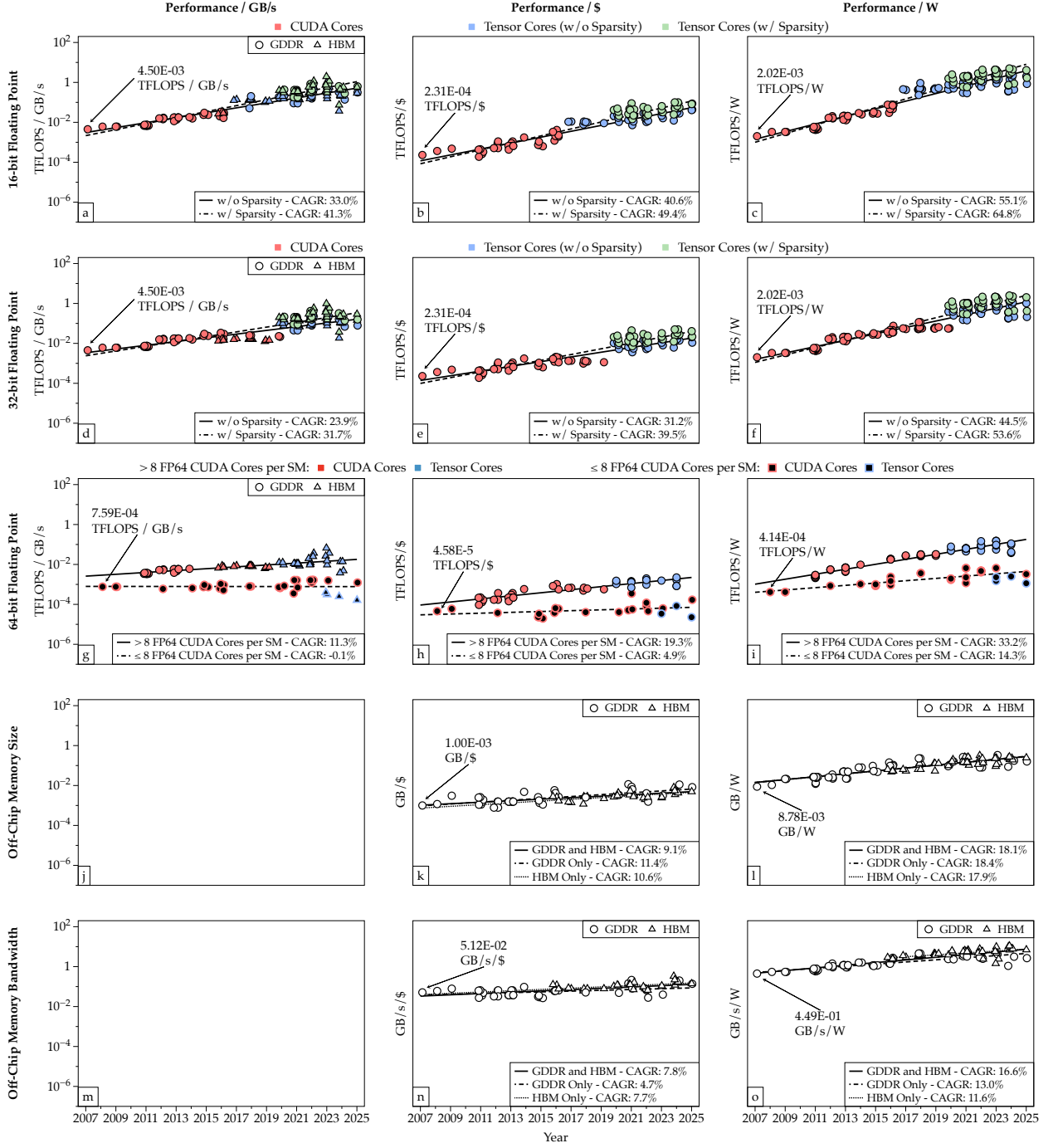


Fig. 5: All datacenter GPUs: Exponential scaling trends for the technical improvements per memory bandwidth (left column), per dollar (central column), and per watt (right column). We apply horizontal jitter to prevent overplotting.

the performance boost that Tensor Cores and sparsity support provide. The Tensor Core contribution is particularly evident in the FP32 per-memory bandwidth trends (CAGRs of 23.9% without sparsity and 31.7% with sparsity), as the scaling of this metric with CUDA Cores (red points) plateaued before the introduction of Tensor Cores. Finally, the two trend lines for the FP64 per-memory bandwidth ratios exhibit intriguing results. While GPUs with a high number of FP64 CUDA Cores and consequently good computational capabilities yield an 11.3% CAGR and 6.46y DT (solid line in Figure 5g), the

other subset of GPUs shows a decreasing trend (dashed line in Figure 5g), suggesting that memory bandwidth outpaces the performance delivered by this configuration.

The central column of plots in Figure 5 reports the technical improvements per dollar. Since the growth of release prices is not as significant as that of off-chip memory bandwidth (see Figure 4), these trends generally yield better CAGRs than those observed in the left column of plots in Figure 5. In particular, the trends in computational performance for FP16 and FP32 indicate CAGRs of 40.6% (49.4% with sparsity) and

31.2% (39.5%), respectively, roughly 7 PPTs higher than those observed in the per-memory bandwidth ratios. In addition, both subsets of GPUs, based on the number of FP64 CUDA Cores per SM, show positive growth trends, even though the growth for low FP64 capabilities is relatively slow (4.9% CAGR and 14.36y DT). Moving to off-chip memory, it is interesting to note that the three trend lines for each metric (memory size and bandwidth) almost overlap. Indeed, these per-dollar ratios significantly reduced the gap and contribution of HBM technology we highlighted in Figure 4, mainly due to the higher release price of HBM-equipped GPUs. Consequently, the CAGRs range from 9.1% (GDDR and HBM) to 11.4% (GDDR only) for off-chip memory size and from 4.7% (GDDR only) to 7.8% (GDDR and HBM) for bandwidth.

Finally, we discuss the technical improvements per watt (right column of plots in Figure 5). The TDP growth varies less with computational performance across different precisions than the release price and off-chip memory. Therefore, the resulting trends for FP16, FP32, and FP64 are just 5.8 (≤ 8 of FP64 CUDA Cores per SM) to 7.2 (FP16 with sparsity) PPTs away from those in Figure 4, implying DTs ranging from 1.38 to 5.19 years. On the other hand, we again notice a narrow gap between the configurations we selected for the metrics based on off-chip memory size and bandwidth. Generally, HBM-based GPUs have higher TDPs than GDDR-based ones (compensating for higher memory size and bandwidth), which explains why the separate CAGRs for GDDR and HBM are so close. Instead, the joint contribution of GDDR and HBM yields CAGRs that are both between and higher than the separate ones for the off-chip memory size and bandwidth metrics, respectively. This result further demonstrates how HBM has contributed to the progress in both off-chip memory size and bandwidth since its introduction in NVIDIA GPUs, as previously mentioned in § IV-A1, paving the way for a more effective execution of memory-intensive workloads.

C. Trend Comparison

We now compare the trends identified in both the top-GPU-per-year subset and the full dataset of datacenter GPUs. Figure 1 summarizes the CAGRs with 90 percent confidence intervals and DTs for technical, per-memory bandwidth, per-dollar, and per-watt improvements for top-performing GPUs (left side of the chart) and all datacenter GPUs (right side). In addition, Table III presents the main statistics for the data used in our trend analysis, including sample size, mean, standard deviation, and R^2 .

Starting with the technical improvements, the subset of top-performing GPUs reports higher CAGRs than the whole dataset of datacenter GPUs across all considered configurations, except for one (i.e., > 8 FP64 CUDA Cores per SM), even though the CAGRs are pretty close. Specifically, computational performance metrics are apart by 6.4, 6.4, and 0.1 PPTs for FP16, FP32, and FP64, respectively. The gaps between the two sets of GPUs are slightly bigger when considering the off-chip memory size (6.5 PPTs) and bandwidth (7.6 PPTs) metrics. Finally, the subset of top-performing GPUs increases the CAGRs for release price and TDP by $1.57\times$

and $1.93\times$ (or decreases the DTs by $0.66\times$ and $0.53\times$), respectively. These results align with our expectations, showing that best-in-class GPUs better reflect the steeper growth in such metrics, even when this outcome implies higher prices or power consumption than the other GPUs from the same period of time.

In terms of per-memory bandwidth, per-dollar, and per-watt ratios, however, we observe a quite different scenario: most metrics yield lower CAGRs when restricting the analysis to the subset of top-performing GPUs. In general, this outcome occurs because top GPUs usually feature off-chip memory with higher bandwidth and are the most expensive and power-hungry, as the mean statistic indicates in Table III, offsetting the performance advantages reflected in the base metric. For instance, when we analyze the technical improvement per memory bandwidth, the CAGRs range from 30.2% to 7.2% for the top-performing GPUs and from 41.3% to -0.1% for the datacenter GPUs, creating a gap ranging from 2.2 to 4.1 PPTs in favor of the whole GPU dataset across the shared configurations (i.e., FP16 and FP32 without sparsity and FP64 with > 8 FP64 CUDA Cores per SM). Besides, we observe a gap spanning from 2.7 to 5.9 PPTs for CAGRs (or 0.21 to 4.66 years for DTs) when focusing on technical improvement per dollar, another case where the entire GPU dataset exhibits better trends. Finally, the analysis of technical improvement per watt showcases mixed results. Specifically, the subset of top-performing GPUs shows better trends for FP32 and memory size and bandwidth, whereas the complete datacenter GPU dataset shows higher CAGRs for FP64. In addition, both sets yield the same CAGRs for FP16.

V. EXPORT CONTROL REGULATIONS

As discussed in § IV, the computing and memory performance of NVIDIA GPUs has been growing at impressive rates, addressing the ever-increasing demand for performance. This need for computing power is particularly evident in training and inference for large, modern AI models [56]–[58], and is driven by intense competition between both companies and countries in developing the best models and reaching “AI supremacy” [59]–[61]. Given the critical role of GPUs in this geopolitical competition, the United States has recently begun to implement controls on the export of the Integrated Circuits (ICs) designed and produced by U.S. companies on national security grounds – to constrain advances in military and commercial systems fielded by potential adversary countries. In this section, we first provide an overview of recent export control regulations implemented by the United States. We then analyze the implications of these regulations on exports of the GPUs in our dataset, and the potential resulting performance gaps that denial might create.

A. United States Export Control Regulations: Overview

In October 2022, the Bureau of Industry and Security (BIS) within the United States Department of Commerce introduced the first regulation to control and restrict the export of high-performance AI chips to China [4]. Specifically, the regulation added a new Export Control Classification Number (ECCN)

TABLE III: Statistics on the data used to fit the exponential models on the technical improvements per metric and their per-memory bandwidth, per-dollar, and per-watt ratios for top-performing GPUs and all datacenter GPUs

Metric	Configuration	Unit	Top-Performing GPUs						All Datacenter GPUs					
			Sample Size	Mean	Std	Min	Max	R ²	Sample Size	Mean	Std	Min	Max	R ²
Technical Improvement														
16-bit Floating Point	w/o Sparsity	TFLOPS	18	410.49	728.28	0.35	2250	0.98	101	246.31	428.77	0.35	2250	0.90
	w/ Sparsity		-	-	-	-	-	-		473.30	864.90	0.35	4500	0.92
32-bit Floating Point	w/o Sparsity	TFLOPS	18	198.16	367.38	0.35	1125	0.96	101	116.22	216.09	0.35	1125	0.87
	w/ Sparsity		-	-	-	-	-	-		228.46	434.15	0.35	2250	0.88
64-bit Floating Point	> 8 FP64 CUDA Cores per SM	TFLOPS	12	19.88	22.93	0.67	66.91	0.94	65	15.35	20.40	0.51	66.91	0.94
	≤ 8 FP64 CUDA Cores per SM		-	-	-	-	-	-		0.60	0.52	6.86E-02	1.97	0.69
Off-chip Memory Size	GDDR and HBM	GB	18	53.64	72.63	1.50	270	0.96	101	38.14	44.89	1.50	270	0.80
	GDDR Only		-	-	-	-	-	-		17.50	17.56	1.50	96	0.75
Off-chip Memory Bandwidth	HBM Only		-	-	-	-	-	-		62.83	54.45	12	270	0.76
	GDDR and HBM	GB/s	18	1793.69	2421.99	76.80	7700	0.98	101	1139.00	1512.36	76.80	7700	0.72
Release Price	GDDR Only		-	-	-	-	-	-		366.89	289.29	76.80	1597	0.68
	HBM Only		-	-	-	-	-	-		2062.18	1839.16	549.10	7700	0.69
Thermal Design Power	-	\$	17	17533.24	16592.09	1300	55000	0.97	68	12253.58	11807.77	1300	55000	0.53
Technical Improvement Per Memory Bandwidth														
16-bit Floating Point	w/o Sparsity	TFLOPS / GB/s	18	0.11	0.11	4.50E-03	0.30	0.94	101	0.14	0.16	4.50E-03	0.98	0.88
	w/ Sparsity		-	-	-	-	-	-		0.26	0.32	4.50E-03	1.96	0.91
32-bit Floating Point	w/o Sparsity	TFLOPS / GB/s	18	4.83E-02	5.35E-02	4.50E-03	0.15	0.86	101	6.49E-02	7.84E-02	4.50E-03	0.49	0.76
	w/ Sparsity		-	-	-	-	-	-		0.12	0.16	4.50E-03	0.98	0.77
64-bit Floating Point	> 8 FP64 CUDA Cores per SM	TFLOPS / GB/s	12	8.93E-03	4.57E-03	3.75E-03	2.00E-02	0.38	65	1.00E-02	9.82E-03	3.29E-03	6.64E-02	0.59
	≤ 8 FP64 CUDA Cores per SM		-	-	-	-	-	-		9.00E-04	4.50E-04	1.62E-04	1.66E-03	0.00
Technical Improvement Per Dollar														
16-bit Floating Point	w/o Sparsity	TFLOPS / \$	17	1.23E-02	1.52E-02	2.31E-04	5.00E-02	0.94	68	1.14E-02	1.35E-02	1.88E-04	5.00E-02	0.90
	w/ Sparsity		-	-	-	-	-	-		2.13E-02	2.77E-02	1.88E-04	0.10	0.92
32-bit Floating Point	w/o Sparsity	TFLOPS / \$	17	5.60E-03	7.72E-03	2.31E-04	2.50E-02	0.87	68	5.32E-03	6.52E-03	1.88E-04	2.50E-02	0.87
	w/ Sparsity		-	-	-	-	-	-		1.01E-02	1.34E-02	1.88E-04	5.00E-02	0.87
64-bit Floating Point	> 8 FP64 CUDA Cores per SM	TFLOPS / \$	11	8.55E-04	5.05E-04	2.18E-04	1.99E-03	0.61	43	7.20E-04	5.73E-04	9.39E-05	2.23E-03	0.82
	≤ 8 FP64 CUDA Cores per SM		-	-	-	-	-	-		6.79E-05	7.00E-05	1.98E-05	3.49E-04	0.12
Off-chip Memory Size	GDDR and HBM	GB / \$	17	2.59E-03	1.28E-03	1.00E-03	4.91E-03	0.39	68	3.07E-03	2.27E-03	7.79E-04	1.16E-02	0.46
	GDDR Only		-	-	-	-	-	-		2.98E-03	2.68E-03	7.79E-04	1.16E-02	0.51
Off-chip Memory Bandwidth	HBM Only		-	-	-	-	-	-	27	3.21E-03	1.50E-03	1.18E-03	8.00E-03	0.42
	GDDR and HBM	GB/s / \$	17	8.39E-02	3.45E-02	3.56E-02	0.17	0.46	68	8.51E-02	5.54E-02	2.67E-02	0.33	0.40
	GDDR Only		-	-	-	-	-	-		6.29E-02	4.20E-02	2.67E-02	0.21	0.17
	HBM Only		-	-	-	-	-	-		5.69E-02	6.11E-02	0.33	0.29	
Technical Improvement Per Watt														
16-bit Floating Point	w/o Sparsity	TFLOPS / W	18	0.62	0.81	2.02E-03	2.25	0.96	101	0.59	0.65	2.02E-03	2.50	0.91
	w/ Sparsity		-	-	-	-	-	-		1.10	1.33	2.02E-03	5.00	0.93
32-bit Floating Point	w/o Sparsity	TFLOPS / W	18	0.29	0.41	2.02E-03	1.12	0.96	101	0.27	0.33	2.02E-03	1.25	0.90
	w/ Sparsity		-	-	-	-	-	-		0.52	0.68	2.02E-03	2.50	0.90
64-bit Floating Point	> 8 FP64 CUDA Cores per SM	TFLOPS / W	12	4.34E-02	4.30E-02	2.66E-03	0.15	0.86	65	3.93E-02	3.90E-02	2.09E-03	0.15	0.93
	≤ 8 FP64 CUDA Cores per SM		-	-	-	-	-	-		2.50E-03	1.89E-03	4.14E-04	6.57E-03	0.58
Off-chip Memory Size	GDDR and HBM	GB / W	18	0.10	8.68E-02	8.78E-03	0.27	0.90	101	0.12	0.09E-02	8.78E-03	0.33	0.80
	GDDR Only		-	-	-	-	-	-		8.46E-02	7.55E-02	8.78E-03	0.33	0.76
Off-chip Memory Bandwidth	HBM Only		-	-	-	-	-	-	46	0.15	7.18E-02	4.80E-02	0.32	0.63
	GDDR and HBM	GB/s / W	18	3.43	2.88	0.45	9.85	0.95	101	3.28	2.38	0.45	11	0.76
	GDDR Only		-	-	-	-	-	-		5.11	2.14	1.44	11	0.41

3A090, which imposed distinct conditions that a target advanced IC had to meet simultaneously.¹¹ These conditions can be summarized as follows:

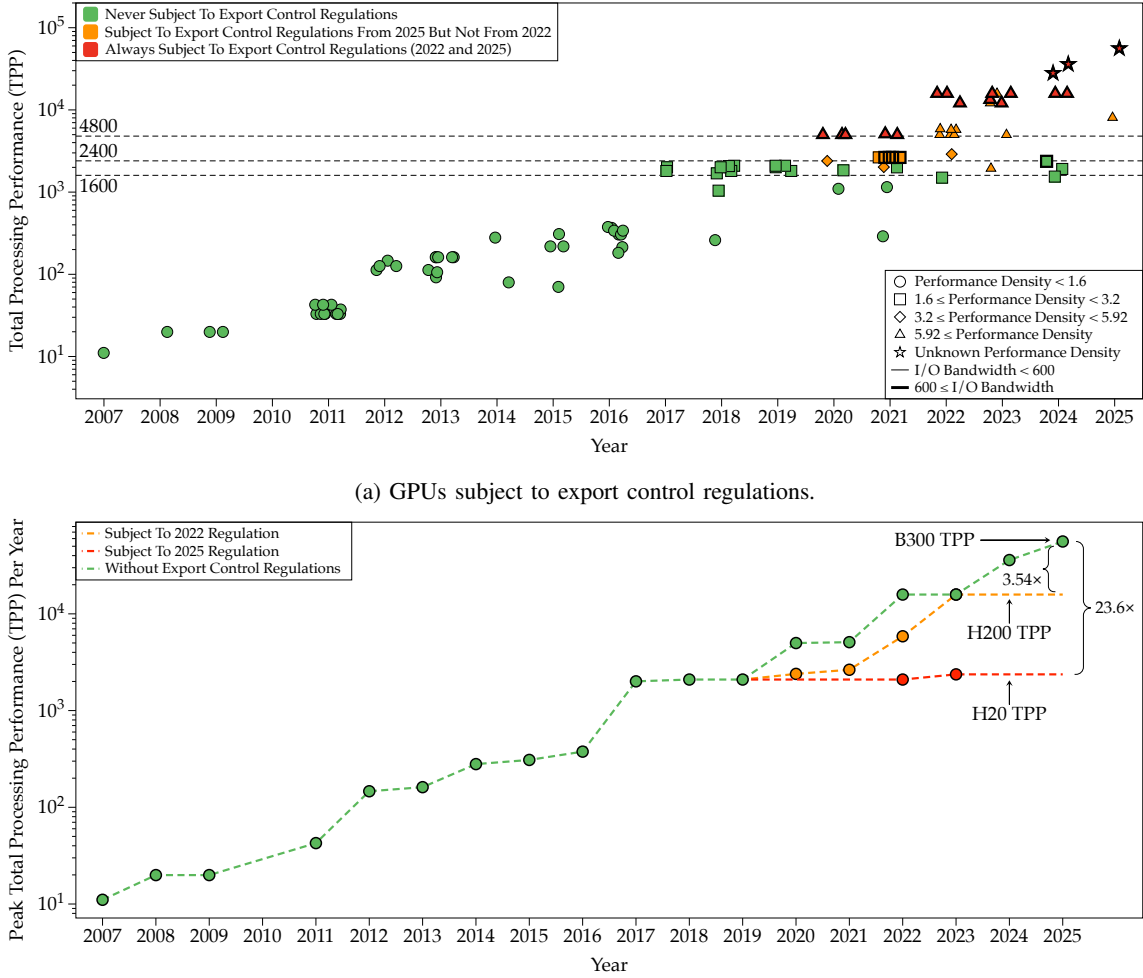
- 1) Aggregate bidirectional Input/Output (I/O) bandwidth ≥ 600 GB/s; and
- 2) Total Processing Performance (TPP) ≥ 4800 .

¹¹The regulation also includes ECCN 4A090, which controls computers, electronic assemblies, and components containing ICs in ECCN 3A090.

The Total Processing Performance (TPP) metric (officially introduced in the following regulations) is defined as:

$$TPP = 2 \cdot MAC_TOPS \cdot b \quad (2)$$

where MAC_TOPS is the number of theoretical peak Tera Operations per Second (TOPS) for Multiply–Accumulate (MAC) computation, and b is the bitwidth of the operation (TFLOPS was used as a performance metric in the previous sections and is $2 \cdot MAC_TOPS$ for FP processing cores). If an IC can support various bit lengths that achieve different TPP



(b) Peak exportable Total Processing Performance (TPP) per year with and without export control regulations (we depict a non-decreasing pattern for each curve, meaning we keep the current maximum TPP over the years, even if the TPP in a subsequent year is lower).

Fig. 6: Impact of the United States export control regulations from 2022 and 2025 on the GPUs in our dataset. We first show what GPUs are (or are not) subject to export control based on the regulations from 2022 and 2025. Then, we illustrate how the peak exportable Total Processing Performance (TPP) per year changes when considering no export control regulations or the ones from 2022 and 2025 and the consequent performance gap. We apply horizontal jitter to the data points to prevent overplotting.

values (as in the case of GPU chips), the regulation restricts the highest TPP value. Finally, the TPP values are for processing dense data; hence, we do not account for sparsity, even when supported.

Since this regulation prevented the export of GPUs such as A100 and H100 to China, NVIDIA launched derivative GPUs, namely the A800 and H800 (both in our dataset), to comply with the U.S. regulations while still serving the Chinese market. These GPUs incorporate chips that are basically identical to their non-export-controlled counterparts but reduce I/O bandwidth (A800 and H800) and/or FP64 performance (H800). A later 2023 revised regulation further tightened the restrictions and banned the export of these GPUs as well [5]. Similarly, another regulation from 2024 [6], [7] expanded the control scope to off-chip memories on GPU modules and included an additional constraint on HBM density on

exportable chips.

The latest regulation, announced in January 2025, is part of a ‘Framework for Artificial Intelligence Diffusion’ [8], further expanding existing export restrictions on high performance computing devices and HBM-based memory chips under ECCN 3A090. In particular, ECCN 3A090 features three distinct performance criteria:

- 3A090.a controls ICs having either:
 - 1) $\text{TPP} \geq 4800$; or
 - 2) $\text{TPP} \geq 1600$ and performance density ≥ 5.92 ;
- 3A090.b controls ICs having either:
 - 1) $2400 \leq \text{TPP} < 4800$ and $1.6 \leq \text{performance density} < 5.92$; or
 - 2) $\text{TPP} \geq 1600$ and $3.2 \leq \text{performance density} < 5.92$.
- 3A090.c controls HBM-based memory chips having

memory bandwidth density > 2 GB/s per mm².

Performance density is defined as the ratio between TPP and the die area of a given AI chip, whereas memory bandwidth density is the memory bandwidth divided by the area of the memory package or stack. It is important to note that advanced computing ICs that include co-packaged logic and HBM are not controlled by 3A090.c, even though they may be controlled by other ECCNs (e.g., 3A090.a or 3A090.b) based on their TPP and performance density. Finally, ECCN 4A090 regulates the export of computers, electronic assemblies, and components that incorporate the aforementioned ICs.

Under the 2025 regulation, the top-performing GPUs that NVIDIA could export were the Ada L2 and L20 and the Hopper H20, mainly designed for export purposes [62]. However, after the U.S. approved the export of the H200 to “approved customers” worldwide (on the condition that the U.S. collects a 25% fee on the sales), this device has become the top-performing exportable NVIDIA GPU [63], [64].

B. United States Export Control Regulations: Implications

Having summarized evolving U.S. export control regulations, we can now analyze their potential impact on the GPU landscape. Specifically, we want to examine how such regulations affect the export of GPUs in our dataset and the potential performance gap that may arise between the United States and target countries. Consequently, we evaluate the first regulation from 2022 through the last one from 2025. To this end, we employ the metrics available in our dataset, namely the peak computational performance (usually delivered by Tensor Cores), die size, and NVLink bandwidth, to evaluate the criteria based on TPP, performance density, and aggregated I/O bandwidth. Lacking published public data on the die area of packaged HBM memory devices, we mainly ignore the parts of the 2024 and 2025 regulations covering HBM in our analysis, which would not prevent the export of advanced computing ICs anyway, as mentioned before. Nonetheless, we note that exports of HBM chips conforming to the non-proprietary, 8-year-old international JEDEC standard HBM2 generally seem to be permitted, while chips meeting the newer JEDEC standards for the HBM2e and higher-performing standards (HBM3, HBM3e, HBM4) are generally restricted [65].

Figure 6 shows the impact of the United States export control regulations in 2022 and 2025 through two charts. Figure 6a highlights how these regulations affect the export of the GPUs in our dataset and indicates the various TPP (dotted lines), performance density (point shapes), and I/O (point border thickness) thresholds employed in the two target regulations. Specifically, we can observe that no GPU released prior to 2019 is subject to either regulation, while most GPUs from 2020 and later are subject to export control regulations due to either the initial 2022 criteria or the more stringent criteria enacted in 2022 and 2025. Figure 6b shows the consequences of such regulations, with lines indicating the peak TPP per year and how values change (or remain constant) under no export control regulations (green), the 2022 regulations (orange), and the 2025 regulations (red). This Figure does not show trends but rather absolute/punctual peak

TPP values per year, and marks the B300 as the GPU with the highest currently available TPP in the U.S. territory. The outcome is a maximum $3.54\times$ and $23.6\times$ performance gap in computing power (measured as TPP) separating countries not subject to export control regulations from those subject to the 2022 and 2025 regulations, respectively, indicating how the 2025 regulations are much more restrictive than those from 2022. If we account for the U.S. agreement on the export of the H200 [63], [64] in December 2025, the new potential gap drops to $3.54\times$, which is interestingly equivalent to the gap we observed under the 2022 regulation. Generally, the 2025 controls effectively restrict GPU performance to levels surpassed in 2020 (or in 2024, if we consider the recent policy update). These controls do not account for other metrics such as off-chip memory size and bandwidth, which are particularly relevant in the AI field, the primary focus of these regulations. Our estimations of the performance gap assume that the export controls are effective and that comparable GPU devices are not developed and sold by companies not subject to U.S. export controls.

Another way to analyze the impact of U.S. export control regulations is to look at the potential gap in terms of TPP/\$. If we consider the B300, H20, and H200 GPUs (i.e., the GPUs with the highest TPP in the U.S., exportable under the 2025 regulations, and exportable after the recent policy update, respectively), we can observe that the initial gap between B300 and H20 in TPP/\$ was $5.16\times$. However, this gap shrinks to $2.57\times$ when replacing H20 with H200, implying that foreign countries can now potentially access $2\times$ more TPP for the same investment.

Finally, despite this theoretical potential performance gap and consequent technological retardation, we should consider that these restrictions create powerful incentives to develop alternative technologies on the part of sanctioned countries, and stimulate creativity in both technological approaches, with researchers pursuing alternative innovative solutions and optimizations to keep pace with competitors, as well as creative ways to covertly bypass restrictions [66]. The recent release of AI models by the Chinese firm DeepSeek is an example of countering restrictions with innovation [67], [68]; specifically, DeepSeek is reported to have relied on a few thousand H800 GPUs and implemented various optimization techniques to improve pipeline and data parallelism, counterbalancing the bandwidth limitations of the GPU utilized. Chinese memory producers are already producing their own HBM2 chips, have announced plans to ship HBM3 chips by 2026, and are rapidly narrowing their lag behind the US and Korean memory chip producers at the current leading edge of memory chip innovation [69], [70]. Furthermore, Chinese chip makers are currently producing homegrown GPU designs (such as Huawei’s Ascend 910C, the best domestically produced Chinese AI chip [71], [72]) that, while not as performant as top NVIDIA designs, could close the gap in the future [69]. However, the current production capacity of Chinese companies like Huawei is a small fraction of NVIDIA’s (5.3% in 2025 and expected to drop to 2.2% in 2027 [72]); therefore, allowing China access to performant GPUs like the H200 (which is marginally more powerful than the Huawei Ascend 910C in computational per-

formance and memory size/bandwidth) could increase China’s ability to build and deploy large, cutting-edge AI models.

Historically, export controls have met with limited long-run success in halting the eventual international diffusion of technology. The classic example is British export restrictions on textile machinery and knowhow during the first industrial revolution, which were wholly unsuccessful in preventing the diffusion of these technological innovations to rival industries in the United States and continental Europe, before they were abolished in the middle of the nineteenth century [73]–[75]. While undoubtedly making GPU compute acquisition more difficult and costly in the short term for geopolitical rivals, there is little current or historical evidence that suggests that any “performance gap” resulting from these controls is likely to persist for long. Economic history instead suggests that investment in continued innovation at the technological frontier is likely to be a more successful strategy to maintain technological leadership [76]–[80]. While lower cost strategies to quickly copy innovations and profitably follow a leader have at times been successful, it is difficult to see how technological leadership can be sustained without significant investments in frontier research and development. The current competitive dynamics of global R&D investments in AI computing hardware would seem to support this thesis.

VI. RELATED WORK AND LIMITATIONS

This section first reports similar relevant studies in the literature and compares them with our analysis. The section then examines the limitations of our work and suggests possible prospective research opportunities.

A. Related Work

The literature already contains studies and observations that aim to identify progress in GPUs (especially NVIDIA ones) from different perspectives. Probably the most widely-known example is Huang’s law [9], [18], [24], [81], named after Jensen Huang, president and CEO of NVIDIA. This empirical law, which can be considered the counterpart of Moore’s law for GPUs, has undergone several iterations as NVIDIA has released new GPUs and has reported AI compute gains over the years. Specifically, this law focuses on the peak theoretical performance each NVIDIA GPU microarchitecture can deliver for AI computations at the lowest supported data precision. If a given GPU does not support that specific precision (e.g., FP4), this law relies on performance at higher precisions (e.g., 8 or 16 bits). The iteration of Huang’s law presented at COMPUTEX 2024 [81] spans from 2016 (19 TFLOPS FP16, Pascal P100) to 2024 (20,000 TFLOPS FP4 with sparsity, Blackwell B200) and reports a $1000 \times$ AI compute gain over 8 years.

Huang’s law provides a limited approach to GPU progress trends because it considers only the peak computing performance of 5 GPUs or microarchitectures [81] (missing many years and devices) and combines different levels of data precision. Combining bitwidths in this way is questionable as a matter of historical progress, but is certainly incorrect if we want to predict future progress, since it is implausible from

TABLE IV: Comparison of the yearly FP16 and FP32 improvements rates between our work and Epoch AI’s

Metric	Progress [%]		Progress / \$ [%]	
	Ours	Epoch AI	Ours	Epoch AI
16-bit Floating Point (w/o Sparsity)	62	36	33	30
16-bit Floating Point (w/ Sparsity)	72	NA	41	NA
32-bit Floating Point (w/o Sparsity)	51	28	24	30
32-bit Floating Point (w/ sparsity)	60	NA	32	NA

both physical and functional perspectives that bitwidths can continue to decrease¹². Consequently, Huang’s law yields an overestimated CAGR of 138% (or DT of 0.8 years), which is 66 PPTs higher than the best CAGR we identified in our analysis (i.e., FP16 with sparsity for all datacenter GPUs). Unlike Huang’s law, our work also provides a comprehensive analysis spanning a longer period, includes 101 NVIDIA GPUs, covers multiple key metrics, and is more consistent across different data-precision levels.

Epoch AI has also done two studies, one in 2023 and one in 2024, analyzing progress in ML hardware [25], [26]. As shown in Table IV, we find substantially different growth rates of progress than they do. These differences arise for two reasons: (1) Epoch AI’s analyses are much more heterogeneous, covering 170 devices. This approach gives those other devices more weight in the trend, whereas ours focuses on the standard and most-common architecture for ML and AI, NVIDIA datacenter GPUs. (2) Epoch AI also chooses to group devices differently than we do. Specifically, they separate out traditional (e.g., CUDA) and tensor performance and analyze them separately. We instead pool these into a single analysis, because they compete for the same space on the chip and thus a decrease in one (e.g., FP64 CUDA Cores) can be used to get more of the other (Tensor Cores), as in the Blackwell Ultra B300.

Our analysis also considers important characteristics that Epoch AI misses, for instance, we account for sparsity in processor capabilities, measure FP64 performance improvement, and we track how computing performance is growing relative to off-chip memory bandwidth, which is crucial for understanding whether calculations will be bottlenecked by a “memory wall” [55].

In summary, our work focuses on making apples-to-apples comparisons of the main processors used in AI by the dominant vendor of those processors. Within this set, we provide a comprehensive and consistent analysis spanning multiple metrics and configurations to assess various kinds of progress trends. Our work also includes an analysis of the potential impact of U.S. export control regulations on accessible GPU performance and the resultant capability gaps they may create.

B. Limitations

Although we believe this analysis offers an objective overview of the current pace of progress in NVIDIA GPUs, we believe there is still room for improvement. First, one of

¹²Our work might seem to have a similar bias from GPUs before 2016, since we use their 32-bit performance, but this is because that is how those chips emulated 16-bit precision. We do not assume that bitwidths can continue declining.

the most cumbersome parts of our analysis was GPU release price data collection. Top-notch datacenter GPUs are primarily purchased by corporate customers and authorized distributors, who often negotiate bulk deals that may include specific customizations. Typically, NVIDIA does not provide an official retail price in its announcements for such high-end devices, making the concept of a “release price at launch” more of a theoretical economic notion rather than an officially published number. Consequently, data collection was not straightforward or exhaustive, and we could not find precise information for all the GPUs reported in Table I and their variants, leading us to drop roughly one-third of the GPUs from our per-dollar analysis (Table III).

Next, the discussion about the CAGRs and doubling times in § IV is based solely on high-level metrics such as peak performance at different precisions. Effectively we are just observing the outcomes of enhancements occurring at the hardware level. A low-level analysis focusing on changes in the area and functionality of computing and on-chip memory components (i.e., caches) could unveil further insights about both past/current progress of GPUs and future potentially productive directions. Of course, such an analysis would require access to hardware design details that vendors do not tend to share publicly, as this could undermine their competitive advantage. While entities such as TechInsights, SemiAnalysis and Locuza publish articles [82]–[84] that uncover the architectural specifications of some GPU chips, the limited number of GPUs examined hinders a more comprehensive analysis.

Another direction for analysis would be to distinguish between the physical design features of a given chip and the variants of those features actually sold in commercially available GPUs. In other words, even though the same chip design die model (same die size and transistor count) is used across multiple GPU boards, each device sold typically implements only a subset of the full theoretical capabilities fabricated in the die model. For instance, the GH100 GPU chip includes 18432 FP32 CUDA Cores in its full implementation [43]. However, all the Hopper GPU boards reported in this study, based on the same chip, have either 16896 or 14592 FP32 CUDA Cores, depending on the form factor. The difference between capabilities in actual models sold and those available theoretically in the chip hardware design is undoubtedly due, to some extent, to design redundancy intended to correct for fabrication defects. By having “spare” CUDA cores available, defective cores can be fused off and replaced with spares, thus increasing the yield rate of good dies on a processed silicon wafer and reducing fabrication cost. This aspect is crucial for NVIDIA GPUs, which are among the largest chips ever manufactured, often as large as the current state of chip fabrication technology permits. Constant defect densities in semiconductor fabrication imply that larger chips will, on average, have more defects. Redundant features turn otherwise defective chips from scrap into saleable products.

Finally, as mentioned previously, our analysis utilizes peak values for performance and bandwidth, and TDP for power consumption. Please note that other literature studies employ the same approach based on theoretical peak values for computational performance and off-chip memory bandwidth, as well

as TDP [24]–[26]. Although this choice permits analysis of ideal/theoretical characteristics of these GPUs, we recognize that further discussion based on real-world benchmarks (and potentially other GPU vendors) would be beneficial for understanding actual workload performance based on the workload type and on the role of software optimizations. Moreover, the theoretical computing performance values reported in NVIDIA documentation are based on the boost clock, which can only be used for a limited time, as it would quickly push the GPU past its TDP and raise the chip’s operating temperature to alarming levels, causing a fast down-clocking. Similarly, TDP is generally around two-thirds of the maximum power draw, meaning it does not represent either peak or average power consumed during a real-world computation workload [51]. Given the extensive analysis required, we plan to pursue additional research employing real benchmark values to more accurately portray trade-offs in design choices addressing different computing application domains (e.g., AI).

VII. CONCLUSION

GPUs have reshaped and are continuing to reshape the fields of computer science and computer architecture. What was initially a supporting device designed to offload graphics processing from the CPU has undoubtedly become even more critical and compelling than the CPU itself, especially for AI. Indeed, NVIDIA GPUs were one of the main drivers of the current AI revolution, and, even though there may be other devices that are more suitable and specialized for AI workloads, such as Google’s TPUs, they remain the state-of-the-art approach for training and inference of AI models, thanks to both their hardware features and software infrastructure. On the hardware side, NVIDIA has applied several improvements and introduced new capabilities to its GPUs over the years. Components like Tensor Cores or, in general, specialized units/accelerators for AI basic computations were then adopted and implemented similarly by other CPU and GPU vendors for their devices, such as Neural Processing Units (NPUs) in Intel CPUs and Matrix Cores in AMD GPUs. The role of GPUs (and AI processors, in general) has been so prominent recently that the U.S. has introduced national security regulations to control their export.

As the demand for computational power continues to grow at a pace never before seen, examining both past and current technical progress is crucial for identifying future limitations in scientific research. For this reason, our work analyzes significant trends in NVIDIA GPUs. Based on our curated dataset of datacenter GPUs released since the mid-2000s, we provide insights about the technical, per-memory bandwidth, per-dollar, and per-watt CAGRs and DTs, foreshadowing expectations for the near future.¹³ We summarize the key insights from the analysis presented in this paper.

Insight 1 - GPU progress surpassed Moore’s Law to keep pace with AI growth: Moore’s Law has long been the primary indicator of progress in semiconductor technology, predicting that the complexity of ICs would double every two years [15],

¹³We plan to release this dataset as part of the MIT Processor Database: <https://processordb.mit.edu>.

with consequent implications on performance growth. While the CPU improvement rate is slowing down [16], the progress of GPUs and, generally, AI hardware is outpacing Moore's Law prediction, as our analysis of past and current trends in NVIDIA datacenter GPUs indicates; for instance, FP16 performance doubles every 1.28 to 1.44 years (with and without sparsity, respectively). In general, the main driver of GPU and specialized hardware progress is the enormous demand for computing required by AI, whose performance and memory requirements are growing at unprecedented rates (e.g., doubling times of 6 to 10 months for computing demand [10], [11] and 30× per year for longest context windows [12]), pushing the production cycles of the semiconductor industry. As a consequence, NVIDIA is implementing architectural trade-offs to provide customers with fast turnaround times for training increasingly large AI models, while deprioritizing features such as high-precision performance (e.g., FP64).

Insight 2 - chip-level enhancements boosted GPU performance: A significant contribution to the progress of NVIDIA GPUs derives from improvements at the chip level. Features such as FP16 hardware support, specialized AI units (e.g., Tensor Cores), and increasingly large single- and multi-die GPUs have certainly paid off as a short-term solution to boost performance and keep pace with increasing computing demand. The future will tell us more about the sustainability of such an approach and its diminishing returns.

Insight 3 - the computing power of FP16 and FP32 doubles in less than 2 years: Our analysis across our entire dataset indicates the doubling times for FP16 and FP32 performance are 1.44y and 1.69y, respectively. As mentioned in the previous insight, this result is a direct consequence of the performance boost yielded by the Tensor Cores since 2017 (for FP16) and 2020 (for FP32). Moreover, the estimated DTs for FP16 and FP32 decrease further when sparsity support is accounted for (1.28y and 1.47y, respectively), although sparsity is not always applicable.

Insight 4 - FP64 compute units are becoming a lower-priority resource: The growth in FP64 performance is not as prominent as the one of FP16 and FP32. NVIDIA usually sacrifices FP64 compute capability in desktop/workstation-oriented GPUs, limiting the number of FP64 units or omitting FP64 support in the Tensor Cores. This decision implies a slower growth rate, as we observed in the configuration with fewer FP64 CUDA Cores per SM (20.1% across the entire dataset). Similarly, even if pure datacenter GPUs used to provide more FP64 units and Tensor Core support (though not as prominent as for other data precisions), their progress trend will probably decrease in the future, as even top-notch GPUs such as the Blackwell Ultra B300 feature limited FP64 computing capabilities, presumably because they are mainly designed for the AI field, which does not require greater precision [47]–[49] (the same may be true also for other scientific fields [85]), making NVIDIA repurpose those transistors to other data precisions.

Insight 5 - HBM boosted off-chip memory size and bandwidth: Off-chip memory characteristics leaped forward with the introduction of HBM technology. While it took HBM longer to outpace GDDR in terms of memory size, it

immediately contributed to the growth of off-chip memory bandwidth, making HBM an essential component of high-end NVIDIA GPUs. Specifically, HBM alone yielded 31.8% and 24.8% CAGRs for off-chip memory size and bandwidth, which are 13.8 and 12.1 PPTs higher than GDDR alone.

Insight 6 - the growth in release price and TDP for best-in-class GPUs is almost 2× that of the datacenter lineup: Release price and, especially, TDP are slower than other metrics in terms of growth, which is a positive outcome. However, the subset of top-performing GPUs per year yields higher growth rates for both release price and TDP (22.9% and 8.5%, respectively) than NVIDIA's overall datacenter GPU lineup (14.6% and 4.4%), suggesting that best-in-class GPUs are becoming increasingly expensive and power-hungry. Supporting evidence for the second point is that GPU power demand now represents approximately 40% of total power usage in AI data centers [86].

Insight 7 - computing power grows faster than off-chip memory bandwidth: The technical improvements per bandwidth tell an interesting story. Both the subset of top-performing GPUs per year and the entire dataset yield generally favorable progress trends for FP16 and FP32 (though not as high as the related performance growth rates): 30.2% and 33% for FP16 and 21.7% and 23.9% for FP32, respectively. These trends imply that the growth of FP16 and FP32 metrics outpaces off-chip memory bandwidth, potentially making it a bottleneck for computations that heavily depend on off-chip data transfers and creating the so-called memory or bandwidth wall. Interestingly, the FP64 technical improvements per bandwidth show a different picture, especially for GPUs with lower FP64 capabilities, whose growth rate is almost 0%, indicating a fairly balanced growth in both FP64 performance and off-chip memory bandwidth. In general, one way to both address the memory wall and increase computational performance is to reduce the data precision, because the same amount of bits/bytes would contain more data, and the compute units would be potentially able to perform more operations per clock cycle (assuming hardware support for a given data precision and proportional performance scaling). On the other hand, such an approach introduces accuracy loss as the bitwidth decreases, also reaching the physical limit set by the number of bits. Furthermore, low data precision requires quantization algorithms that introduce additional overhead and are usually data- and domain-specific.

Finally, another critical factor likely to widen the gap between computing and off-chip memory capabilities is the current shortage of memory chips; indeed, the ever-increasing demand for off-chip memory in AI data centers is creating a supply-and-demand imbalance, leading to higher memory chip prices and a potential slowdown in AI development [87], [88].

Insight 8 - the technical improvement per watt grows faster than the per-dollar one: In terms of technical improvement per dollar and per watt, we observe release price increases resulting in less technical improvement per dollar than per watt, due to the faster growth of release prices over time than TDP. While there was a historical point when we thought of compute costs as dominated by the cost of electricity to run a GPU, we now tend to think of compute

costs as dominated by the purchase or release price, as proved by these trends. Our analysis shows that TFLOPS/W (compute per variable energy cost) increases by $1.3\times$ to $2.9\times$ relative to TFLOPS/\$ (compute capacity per fixed capital cost).

Insight 9 - the recent update to export control regulations reduced the performance gap from $23.6\times$ to $3.54\times$: Finally, our analysis of recent U.S. export control regulations on advanced AI chips identifies a theoretical, potential peak-performance gap, measured in TPP, of $23.6\times$ that might open up between the U.S. and restricted countries if these export controls had their intended effect. However, as the U.S. recently agreed to allow NVIDIA to export the H200 GPUs, this performance gap dropped to $3.54\times$. While the H200 provides marginal gains over Chinese domestic devices (e.g., Huawei Ascend 910C) in terms of computational performance and memory size/bandwidth, this agreement could enable China to improve its ability to build large cutting-edge AI models significantly, thanks to the access to a greater number of GPUs than its domestic production would provide. Allegedly, Chinese companies have already ordered more than 2 million H200 for 2026 [89].

Finally, while our work provides a retrospective analysis of the progress trends of NVIDIA datacenter GPUs released to date, one could question whether the identified trends can be projected into the future. Despite the new GPUs announced by NVIDIA for the following years promise to deliver unprecedented performance [31], we are doubtful that the aforementioned trends will continue at the rates discussed in this paper. The primary rationale for such uncertainty is that many improvements come from short-term solutions that may yield diminishing returns soon (e.g., reducing data precision or multi-die GPUs). For this reason, we plan to discuss the future prospects and the barriers these trends will face in a forthcoming article.

ACKNOWLEDGMENTS

The Authors would like to thank Filippo Carloni, Andrew Lohn, Albert Reuther, Larry Rudolph, and Ana Trišović for their precious feedback and kind support.

REFERENCES

- [1] TOP500, “TOP500 List of June 2025,” <https://top500.org/lists/top500/2025/06/>, 2024, accessed: 2025-11-13.
- [2] EMBL, “The rise of GPU computing in science,” <https://www.embl.org/news/science/the-rise-gpu-computing-science/>, 2018.
- [3] AceCloud, “The Evolution Of The GPU: How It Became The Heart Of AI And ML,” <https://acecloud.ai/resources/blog/the-evolution-of-gpu/>, 2023.
- [4] Bureau of Industry and Security, “Implementation of Additional Export Controls: Certain Advanced Computing and Semiconductor Manufacturing Items; Supercomputer and Semiconductor End Use; Entity List Modification,” <https://www.govinfo.gov/content/pkg/FR-2022-10-13/pdf/2022-21658.pdf>, 2022, accessed: 2025-02-03.
- [5] —, “Implementation of Additional Export Controls: Certain Advanced Computing Items; Supercomputer and Semiconductor End Use; Updates and Corrections,” <https://www.govinfo.gov/content/pkg/FR-2023-10-25/pdf/2023-23055.pdf>, 2023, accessed: 2025-02-03.
- [6] —, “Foreign-Produced Direct Product Rule Additions, and Refinements to Controls for Advanced Computing and Semiconductor Manufacturing Items,” <https://public-inspection.federalregister.gov/2024-28270.pdf>, 2024, accessed: 2025-02-03.
- [7] —, “Additions and Modifications to the Entity List; Removals from the Validated End-User (VEU) Program,” <https://public-inspection.federalregister.gov/2024-28267.pdf>, 2024, accessed: 2025-02-03.
- [8] —, “Framework for Artificial Intelligence Diffusion,” <https://www.govinfo.gov/content/pkg/FR-2025-01-15/pdf/2025-00636.pdf>, 2025, accessed: 2025-02-03.
- [9] W. J. Dally, S. W. Keckler, and D. B. Kirk, “Evolution of the Graphics Processing Unit (GPU),” *IEEE Micro*, vol. 41, no. 6, pp. 42–51, 2021.
- [10] L. Emberson and D. Owen, “Training compute growth is driven by larger clusters, longer training, and better hardware,” 2025, accessed: 2025-12-16. [Online]. Available: <https://epoch.ai/data-insights/training-compute-decomposition>
- [11] J. Sevilla, L. Heim, A. Ho, T. Besiroglu, M. Hobbahn, and P. Villalobos, “Compute trends across three eras of machine learning,” in *2022 International Joint Conference on Neural Networks (IJCNN)*. IEEE, Jul. 2022, p. 1–8. [Online]. Available: <http://dx.doi.org/10.1109/IJCNN55064.2022.9891914>
- [12] G. Burnham and T. Adamczewski, “Llms now accept longer inputs, and the best models can use them more effectively,” <https://epoch.ai/data-i/insights/context-windows>, 2025, accessed: 2026-01-09.
- [13] NVIDIA, “NVIDIA Tesla P100,” <https://images.nvidia.com/content/pdf/tesla/whitepaper/pascal-architecture-whitepaper.pdf>, 2016, accessed: 2024-12-17.
- [14] G. E. Moore, “Cramming more components onto integrated circuits, reprinted from electronics, volume 38, number 8, april 19, 1965, pp.114 ff,” *IEEE Solid-State Circuits Society Newsletter*, vol. 11, no. 3, pp. 33–35, 2006.
- [15] G. E. Moore *et al.*, “Progress in digital integrated electronics,” in *Electron devices meeting*, vol. 21. Washington, DC, 1975, pp. 11–13.
- [16] T. N. Theis and H.-S. P. Wong, “The End of Moore’s Law: A New Beginning for Information Technology,” *Computing in Science & Engineering*, vol. 19, no. 2, pp. 41–50, 2017.
- [17] C. E. Leiserson, N. C. Thompson, J. S. Emer, B. C. Kuszmaul, B. W. Lampson, D. Sanchez, and T. B. Schardl, “There’s plenty of room at the Top: What will drive computer performance after Moore’s law?” *Science*, vol. 368, no. 6495, p. eaam9744, 2020.
- [18] T. S. Perry, “Move over, Moore’s law. Make way for Huang’s law [Spectral Lines],” *IEEE Spectrum*, vol. 55, no. 5, pp. 7–7, 2018.
- [19] K. Flamm, “Measuring moore’s law: evidence from price, cost, and quality indexes,” in *Measuring and Accounting for Innovation in the 21st Century*. University of Chicago Press, 2021.
- [20] TechPowerUp, “Intel Xeon 6978P,” <https://www.techpowerup.com/cpu-specs/xeon-6978p.c4279>, 2025, accessed: 2026-01-07.
- [21] —, “AMD Ryzen Threadripper PRO 9995WX,” <https://www.techpowerup.com/cpu-specs/ryzen-threadripper-pro-9995wx.c4163>, 2025, accessed: 2026-01-07.
- [22] NVIDIA, “Inside NVIDIA Blackwell Ultra: The Chip Powering the AI Factory Era,” <https://developer.nvidia.com/blog/inside-nvidia-blackwell-ultra-the-chip-powering-the-ai-factory-era/>, 2025, accessed: 2025-11-30.
- [23] CNBC, “NVDA: NVIDIA Corp - Stock Price, Quote and News,” <https://www.cnbc.com/quotes/NVDA>, 2026, accessed: 2026-01-12.
- [24] NVIDIA, “Heeding Huang’s Law: Video Shows How Engineers Keep the Speedups Coming,” <https://blogs.nvidia.com/blog/huang-s-law-daily-hot-chips/>, 2023, accessed: 2024-12-17.
- [25] M. Hobbahn, L. Heim, and G. Aydos, “Trends in machine learning hardware,” 2023, accessed: 2025-12-08. [Online]. Available: <https://epoch.ai/blog/trends-in-machine-learning-hardware>
- [26] Epoch AI, “Data on machine learning hardware,” 10 2024, accessed: 2026-01-17. [Online]. Available: <https://epoch.ai/data/machine-learning-hardware>
- [27] NVIDIA, “NVIDIA BlueField Platform,” <https://www.nvidia.com/en-us/networking/products/data-processing-unit/>, 2025, accessed: 2025-12-16.
- [28] —, “Accelerating Data Center AI with the NVIDIA Converged Accelerator Developer Kit,” <https://developer.nvidia.com/blog/accelerating-data-center-ai-with-the-nvidia-converged-accelerator-developer-kit/>, 2021, accessed: 2025-12-15.
- [29] —, “Converged Accelerators,” <https://www.nvidia.com/content/dam/en-zz/Solutions/gtcf21/converged-accelerator/pdf/datasheet.pdf>, 2023, accessed: 2025-12-15.
- [30] Micron, “The evolution of GDDR: From GDDR1 to GDDR7,” <https://www.micron.com/about/blog/memory/dram/the-evolution-of-gddr-from-gddr1-to-gddr7>, 2024, accessed: 2025-01-29.
- [31] SemiAnalysis, “NVIDIA GTC 2025 - Built For Reasoning, Vera Rubin, Kyber, CPO, Dynamo Inference, Jensen Math, Feynman,” <https://newsletter.semanalysis.com/p/nvidia-gtc-2025-built-for-reasoning-vera-rub>

in-kyber-cpo-dynamo-inference-jensen-math-feynman, 2025, accessed: 2025-12-01.

[32] NVIDIA, “Nvidia gh200 grace hopper superchip,” <https://www.nvidia.com/en-us/data-center/grace-hopper-superchip/>, 2022, accessed: 2025-12-05.

[33] —, “Nvidia gb200 nvl72,” <https://www.nvidia.com/en-us/data-center/gb200-nvl72/>, 2024, accessed: 2025-12-05.

[34] NVIDIA, “Tesla K80 GPU Accelerator,” <https://www.nvidia.com/content/dam/en-zz/Solutions/Data-Center/tesla-product-literature/Tesla-K80-BoardSpec-07317-001-v05.pdf>, 2015, accessed: 2025-11-30.

[35] J. P. Research, <https://www.jonpeddie.com/news/pc-aib-shipments-follow-seasonality-show-nominal-increase-for-q424/>, 2025.

[36] Bloomberg, <https://www.bloomberg.com/news/articles/2025-02-25/about-nvidia-hopper-blackwell-chips-and-why-amd-intel-struggle-to-compete>, 2025.

[37] TechPowerUp, “Ampere Generation,” <https://www.techpowerup.com/gpu-specs/?architecture=Ampere&sort=generation>, 2024, accessed: 2024-12-17.

[38] NVIDIA, “GeForce RTX 30 Series,” <https://www.nvidia.com/en-us/geforce/graphics-cards/30-series/>, 2021, accessed: 2024-12-17.

[39] —, “NVIDIA A100 Tensor Core GPU,” <https://www.nvidia.com/en-us/data-center/a100/>, 2020, accessed: 2024-12-17.

[40] TechPowerUp, <https://www.techpowerup.com>, 2024, accessed: 2024-12-17.

[41] VideoCardz, <https://videocardz.com>, 2024, accessed: 2024-12-17.

[42] NVIDIA, “NVIDIA A100 Tensor Core GPU Architecture,” <https://images.nvidia.com/aem-dam/en-zz/Solutions/data-center/nvidia-ampere-architecture-whitepaper.pdf>, 2020, accessed: 2025-01-07.

[43] —, “NVIDIA H100 Tensor Core GPU Architecture,” <https://resources.nvidia.com/en-us-tensor-core/gtc22-whitepaper-hopper>, 2023, accessed: 2024-12-17.

[44] NVIDIA, “NVIDIA HGX Platform,” <https://www.nvidia.com/en-us/data-center/hgx/>, 2025, accessed: 2025-11-30.

[45] NVIDIA, “NVIDIA Ampere GA102 GPU Architecture,” <https://www.nvidia.com/content/PDF/nvidia-ampere-ga-102-gpu-architecture-whitepaper-v2.pdf>, 2021, accessed: 2025-01-10.

[46] —, “Structured Sparsity in the NVIDIA Ampere Architecture and Applications in Search Engines,” <https://developer.nvidia.com/blog/structured-sparsity-in-the-nvidia-ampere-architecture-and-applications-in-search-engines/>, 2023, accessed: 2025-01-07.

[47] T. Dettmers, M. Lewis, Y. Belkada, and L. Zettlemoyer, “Llm.int8(): 8-bit matrix multiplication for transformers at scale,” 2022. [Online]. Available: <https://arxiv.org/abs/2208.07339>

[48] S. Gupta, A. Agrawal, K. Gopalakrishnan, and P. Narayanan, “Deep learning with limited numerical precision,” 2015. [Online]. Available: <https://arxiv.org/abs/1502.02551>

[49] M. Courbariaux, Y. Bengio, and J.-P. David, “Training deep neural networks with low precision multiplications,” 2015. [Online]. Available: <https://arxiv.org/abs/1412.7024>

[50] NVIDIA, “NVIDIA Blackwell Architecture Technical Brief,” <https://resources.nvidia.com/en-us-blackwell-architecture/blackwell-architecture-technical-brief>, 2025, accessed: 2025-12-10.

[51] J. L. Hennessy and D. A. Patterson, *Computer Architecture, Sixth Edition: A Quantitative Approach*, 6th ed. San Francisco, CA, USA: Morgan Kaufmann Publishers Inc., 2017.

[52] S. Seabold and J. Perktold, “statsmodels: Econometric and statistical modeling with python,” in *9th Python in Science Conference*, 2010.

[53] T. Wright, M. Klein, and J. Wieczorek, “A primer on visualizations for comparing populations, including the issue of overlapping confidence intervals,” *The American Statistician*, vol. 73, no. 2, pp. 165–178, 2019.

[54] NVIDIA, “How to use cuda core and tensor core simultaneously?” <https://forums.developer.nvidia.com/t/how-to-use-cuda-core-and-tensor-core-simultaneously/223881>, 2022, accessed: 2025-01-07.

[55] B. M. Rogers, A. Krishna, G. B. Bell, K. Vu, X. Jiang, and Y. Solihin, “Scaling the bandwidth wall: challenges in and avenues for cmp scaling,” *SIGARCH Comput. Archit. News*, vol. 37, no. 3, p. 371–382, Jun. 2009. [Online]. Available: <https://doi.org/10.1145/1555815.1555801>

[56] M. Shoeybi, M. Patwary, R. Puri, P. LeGresley, J. Casper, and B. Catanzaro, “Megatron-lm: Training multi-billion parameter language models using model parallelism,” 2020. [Online]. Available: <https://arxiv.org/abs/1909.08053>

[57] J. Kaplan, S. McCandlish, T. Henighan, T. B. Brown, B. Chess, R. Child, S. Gray, A. Radford, J. Wu, and D. Amodei, “Scaling laws for neural language models,” 2020. [Online]. Available: <https://arxiv.org/abs/2001.08361>

[58] C. B. Richards, T. W. Baumgarte, and S. L. Shapiro, “Relativistic bondi accretion for stiff equations of state,” *Monthly Notices of the Royal Astronomical Society*, vol. 502, no. 2, p. 3003–3011, Jan. 2021. [Online]. Available: <http://dx.doi.org/10.1093/mnras/stab161>

[59] G. Allison and E. Schmidt, *Is China beating the US to AI supremacy?* Harvard Kennedy School, Belfer Center for Science and International Affairs, 2020.

[60] E. H. Christie, C. Buts, and C. Du Bois, “America, china, and the struggle for ai supremacy,” in *24th Annual International Conference on Economics and Security*, Volos, Greece, 2021.

[61] Medium, “The AI Superpower Showdown,” <https://medium.com/@mcraddock/inside-the-us-china-race-for-technological-supremacy-52cb5c3df063>, 2025, accessed: 2025-02-08.

[62] SemiAnalysis, “Nvidia’s New China AI Chips Circumvent US Restrictions — H20 Faster Than H100 — Huawei Ascend 910B,” <https://news.letter.semianalysis.com/p/nvidias-new-china-ai-chips-circumvent>, 2023.

[63] CNBC, “Trump greenlights Nvidia H200 AI chip sales to China if U.S. gets 25% cut, says Xi responded positively,” <https://www.cnbc.com/2025/12/08/trump-nvidia-h200-sales-china.html>, 2025.

[64] Reuters, “US to allow Nvidia H200 chip shipments to China, Trump says,” <https://www.reuters.com/world/china/us-open-up-exports-nvidia-h200-chips-china-semafor-reports-2025-12-08/>, 2025.

[65] Morgan, Timothy P., “US Curbs HBM Exports to China—More for the Rest of Us,” <https://www.nextplatform.com/2024/12/02/us-curbs-hbm-exports-to-china-more-for-the-rest-of-us/>, 2024, accessed 2025-05-22.

[66] T. Hwang and E. S. Weinstein, *Decoupling in strategic technologies: From satellites to artificial intelligence*. Center for Security and Emerging Technology, 2022.

[67] D. Guo, Q. Zhu, D. Yang, Z. Xie, K. Dong, W. Zhang, G. Chen, X. Bi, Y. Wu, Y. Li *et al.*, “Deepseek-coder: When the large language model meets programming—the rise of code intelligence,” *arXiv preprint arXiv:2401.14196*, 2024.

[68] X. Bi, D. Chen, G. Chen, S. Chen, D. Dai, C. Deng, H. Ding, K. Dong, Q. Du, Z. Fu *et al.*, “Deepseek llm: Scaling open-source language models with longtermism,” *arXiv preprint arXiv:2401.02954*, 2024.

[69] Wang, Ray and Ottinger, Lily, “Mapping China’s HBM Advances,” <https://www.chinatalk.media/p/mapping-chinas-hbm-advancement>, 2025, accessed 2025-05-22.

[70] Min-gyu, Hwang, “YMTc expected to outproduce Micron in NAND flash while SK hynix cuts output,” <https://biz.chosun.com/en/en-it/2025/05/16/17XUWDAC5JACLPTZC4AP725LFU/>, 2025, accessed 2025-05-22.

[71] V. Blabová and R. Rahman, “Why china isn’t about to leap ahead of the west on compute,” 2025, accessed: 2025-12-16. [Online]. Available: <https://epoch.ai/gradient-updates/why-china-isnt-about-to-leap-ahead-of-the-west-on-compute>

[72] Council on Foreign Relations, “China’s AI Chip Deficit: Why Huawei Can’t Catch Nvidia and U.S. Export Controls Should Remain,” <https://www.cfr.org/article/chinas-ai-chip-deficit-why-huawei-cant-catch-nvidia-and-us-export-controls-should-remain>, 2025, accessed: 2025-12-16.

[73] J. R. Harris, *Industrial Espionage and Technology Transfer: Britain and France in the 18th Century*. Routledge, 1998.

[74] D. J. Jeremy, *Transatlantic Industrial Revolution: The Diffusion of Textile Technologies between Britain and America, 1790-1830s*. MIT Press, 1981.

[75] Kelly, Morgan and O’Rourke, Kevin H, “Industrial policy on the frontier: lessons from the first two industrial revolutions,” 2023.

[76] M. Abramovitz, “Catching up, forging ahead, and falling behind,” *The journal of economic history*, vol. 46, no. 2, pp. 385–406, 1986.

[77] D. C. Mowery and N. Rosenberg, *Paths of innovation: Technological change in 20th-century America*. Cambridge University Press, 1999.

[78] J. Mokyr, “The gifts of athena: Historical origins of the knowledge economy,” in *The gifts of Athena*. princeton university press, 2011.

[79] M. Mazzucato, “The entrepreneurial state: Debunking public vs. private sector myths,” 2013.

[80] M. Fleming, *Breakthrough: A Growth Revolution*. Business Expert Press, 2022.

[81] NVIDIA, “Nvidia ceo jensen huang keynote at computex 2024,” <https://www.nvidia.com/en-us/on-demand/session/computex24-keynote/>, 2024, accessed: 2025-12-05.

[82] TechInsights, “NVIDIA Blackwell B200 Processor Floorplan Analysis,” <https://www.techinsights.com/blog/nvidia-blackwell-b200-processor-floorplan-analysis>, 2025, accessed: 2026-01-12.

[83] SemiAnalysis, “Nvidia Ada Lovelace Leaked Specifications, Die Sizes, Architecture, Cost, And Performance Analysis,” <https://www.semianalysis.com/p/nvidia-ada-lovelace-leaked-specifications>, 2022, accessed: 2024-12-17.

- [84] Locuza, "Nvidia's Ada lineup, configurations, estimated die sizes and a comparison with other chips," <https://locuza.substack.com/p/nvidias-a-da-lineup-configurations>, 2022, accessed: 2024-12-17.
- [85] J. Domke, K. Matsumura, M. Wahib, H. Zhang, K. Yashima, T. Tsuchikawa, Y. Tsuji, A. Podobas, and S. Matsuoka, "Double-precision fpus in high-performance computing: an embarrassment of riches?" in 2019 IEEE International Parallel and Distributed Processing Symposium (IPDPS). IEEE, 2019, pp. 78–88.
- [86] L. Emberson and B. Cottier, "GPUs account for about 40% of power usage in AI data centers," 2025, accessed: 2025-12-20. [Online]. Available: <https://epoch.ai/data-insights/gpus-power-usage-in-ai-data-centers>
- [87] Reuters, "The ai frenzy is driving a memory chip supply crisis," <https://www.reuters.com/world/china/ai-frenzy-is-driving-new-global-supply-chain-crisis-2025-12-03/>, 2025, accessed: 2026-01-06.
- [88] I. D. Corporation, "Global memory shortage crisis: Market analysis and the potential impact on the smartphone and pc markets in 2026," <https://www.idc.com/resource-center/blog/global-memory-shortage-crisis-market-analysis-and-the-potential-impact-on-the-smartphone-and-pc-markets-in-2026/>, 2025, accessed: 2026-01-06.
- [89] Reuters, "Exclusive: Nvidia sounds out tsmc on new h200 chip order as china demand jumps, sources say," <https://www.reuters.com/world/china/nvidia-sounds-out-tsmc-new-h200-chip-order-china-demand-jumps-sources-say-2025-12-31/>, 2025, accessed: 2026-01-06.



Emanuele Del Sozzo got his Ph.D. in Information Technology from Politecnico di Milano in 2019. He received his B.Sc. and M.Sc. in Computer Engineering from Politecnico di Milano in 2012 and 2015. In 2015, he also received a M.Sc. degree in Computer Science from the University of Illinois at Chicago (UIC) and an Alta Scuola Politecnica Diploma. He was a Postdoctoral Researcher at IBM Research (2019), Politecnico di Milano (2020-2022), and RIKEN Center for Computational Science (2022-2023). His research focuses on progress trends in computer architectures, reconfigurable systems, and code generation/optimization. He is currently a Research Scientist at the Massachusetts Institute of Technology.

Roundtable. Martin was a former member of the Federal Economic Statistics Advisory Committee and of the Federal Reserve Bank of New York's Fintech Advisory Committee. He is a Fellow of The Productivity Institute and a Fellow of the National Association for Business Economics recognized for outstanding performance as a business economist, contribution to the field of business economics, and service to NABE. Martin is also a consultant to the U.S. Bureau of Economic Analysis. Martin is currently a Research Scientist at MIT Sloan and engaged in MIT's Computer Science and Artificial Intelligence Lab (CSAIL) FutureTech Project at the intersection of economics and computer science.



Martin Fleming holds a B.S. in mathematics from the University of Massachusetts, Lowell and an M.A. and Ph.D. in economics from Tufts University. Martin is the former IBM Chief Economist and Chief Analytics Officer and former Chief Revenue Scientist, Varicent, the Toronto-based sales-performance management software provider. Martin is a member and former chair of the Conference of Business Economists, a participant in the Brookings Productivity Measurement Initiative, and a member of the Federal Reserve Bank of Chicago Economists

Roundtable. Martin was a former member of the Federal Economic Statistics Advisory Committee and of the Federal Reserve Bank of New York's Fintech Advisory Committee. He is a Fellow of The Productivity Institute and a Fellow of the National Association for Business Economics recognized for outstanding performance as a business economist, contribution to the field of business economics, and service to NABE. Martin is also a consultant to the U.S. Bureau of Economic Analysis. Martin is currently a Research Scientist at MIT Sloan and engaged in MIT's Computer Science and Artificial Intelligence Lab (CSAIL) FutureTech Project at the intersection of economics and computer science.



Kenneth Flamm holds a PhD in Economics from MIT and a BA (with Distinction) in Economics (Honors) from Stanford. He was elected in 2016 to membership in the Conference on Research in Income and Wealth. He previously was appointed chair or vice-chair of two National Research Council panels and served as a member of its Science, Technology and Economic Policy Board. He has been a member of six other National Academies panels, and chair of the NATO Science Committee's Science and Technology Policy and Organization panel. He served on the Federal Networking Council Advisory Committee, on the OECD's Expert Working Party on High Performance Computers and Communications, on various federal advisory committees and as a consultant to government agencies, international organizations, and private corporations. Dr. Flamm received the Department of Defense's Distinguished Public Service Medal from the secretary of defense. Dr. Flamm has served as senior fellow in foreign policy studies at the Brookings Institution and as an economics professor at the Instituto Tecnológico Autónomo de México, the University of Massachusetts at Amherst, and George Washington University. Kenneth is Professor Emeritus in the LBJ School of Public Affairs, University of Texas at Austin and Affiliate Professor at MIT FutureTech.



Neil Thompson has a PhD in Business & Public Policy from UC Berkeley, Haas, dual Master degrees' in Computer Science and Statistics from UC Berkeley, and a Masters in Economics from London School of Economics and Political Science (LSE). From his undergraduate studies, Dr. Thompson has Bachelors degrees in Physics, Economics, and International Development studies from Queen's University. Previously, Dr. Thompson served as an Assistant Professor of Innovation and Strategy at the MIT Sloan School of Management, where he co-directed the Experimental Innovation Lab (X-Lab), and as a Visiting Professor at the Laboratory for Innovation Science at Harvard University. Prior to his academic career, Dr. Thompson has held positions for esteemed organizations such as the Broad Institute, Bain and Company, Lawrence Livermore National Laboratory, AMD, the World Bank, the United Nations, and the Canadian Parliament. Dr. Neil Thompson is the Director of the FutureTech research group, and Principle Research Scientist at MIT's Computer Science and Artificial Intelligence Lab (CSAIL), and at MIT's Initiative on the Digital Economy (IDE) within the Sloan School of Management.